THE UNIVERSITY OF ALBERTA

THE RELATION BETWEEN THE NORTH PACIFIC SEA-SURFACE TEMPERATURE ANOMALY DURING THE SIXTIES AND HAIL DAMAGE IN ALBERTA

by

© JOHN DUBLIN

A THESIS

SUBMITTED TO THE FACULTY OF GRADUATE STUDIES AND RESEARCH

IN PARTIAL FULFILMENT OF THE REQUIREMENTS FOR THE DEGREE

OF MASTER OF SCIENCE

DEPARTMENT OF GEOGRAPHY

EDMONTON, ALBERTA

SPRING, 1972

THE UNIVERSITY OF ALBERTA

FACULTY OF GRADUATE STUDIES AND RESEARCH

The undersigned certify that they have read, and recommend to the Faculty of Graduate Studies and Research, for acceptance, a thesis entitled "The Relation Between the North Pacific Sea-Surface Temperature Anomaly During the Sixties and Hail Damage in Alberta", submitted by John Dublin in partial fulfilment of the requirements for the degree of Master of Science.

ABSTRACT

This study examines the effect of the anomalous sea-surface temperature regime in the North Pacific during the period 1962-67, on hail damage in Alberta, Canada. Thirty-three years of hail insurance records are used to investigate the problem. The extent of the change in the upper air circulation is examined by means of objective analysis of monthly mean upper air data. Quasi-meridional cross-sections are constructed through the hail area using winds calculated from the height fields produced by the objective analysis.

Hail damage in Alberta, as indicated by loss to risk ratios, is reduced considerably during the anomalous period. Analysis of the monthly mean cross-sections reveals a significant change in the upper air circulation during this period. The mean jet stream is found to be further south and much more intense than for the period 1950-61.

Correlation of annual loss to risk ratios with monthly mean meteorological variables, such as wind speed, direction, and shear over the hail area in Alberta failed to establish any connection. A commonly held belief that high spring rainfall leads to heavy summer hail damage is disproved using the hail insurance data and monthly mean precipitation figures for three river basins.

DEDICATION

This thesis is dedicated

to my loving wife Sharon

and son Ian

ACKNOWLEDGEMENTS

I am grateful to a number of people without whose assistance this study could not have been completed.

I wish to thank Dr. E. P. Lozowski, who served as my departmental supervisor, for his suggestions, assistance, and thorough review of the manuscript. I am grateful to Dr. P. W. Summers for his many ideas and injections of enthusiasm. Prof. R. W. Longley kindly served as a sounding board for many of the ideas and helped bring some of the results into perspective. Dr. U. M. Von Maydell must be thanked for her willingness to serve on the examining committee.

The hail insurance data used in this thesis was provided by the Alberta Hail Studies section of the Research Council of Alberta. Mr. L. Wojtiw wrote the program that calculated the loss to risk ratios for the river basins. The precipitation data used was furnished by Prof. R. W. Longley. The upper air data used was extracted, key punched, and verified by my wife Sharon, who also typed the first draft. Mrs. Laura Smith is commended for her efficient typing of the manuscript.

I wish to express my appreciation to the technical staff of the Department of Geography for their suggestions during the drafting of the illustrations, and the photographic reduction of the finished products.

This study was undertaken while I was on educational leave from the Atmospheric Environment Service of the Department of the Environment.

TABLE OF CONTENTS

LIST OF TABLES

LIST OF FIGURES

CHAPTER 1

AIR-SEA INTERACTIONS

1.1 Introduction

Meteorologists have long been aware of the importance of the large scale interactions between the vast water surfaces of the earth and the atmosphere. The ocean surfaces between the great westerly belts are the major source of the heat that drives the 'atmospheric engine'. The peculiarities of many climates have been ascribed to the proximity to a certain body of water or the circulation therein.

Variations in sea surface temperature cause subsequent variations in the general circulation of the atmosphere and vice versa. However, the response of the atmosphere to changes in sea surface temperature is relatively rapid, but the converse is not. Oceanic circulations are quite sluggish and have very large time constants compared to those for the atmosphere.

1.2 Milestones in Teleconnection

The effect of large scale air-sea interactions on the climate of a distant area is commonly referred to as teleconnection. The pioneering work in this field was carried out by Helland-Hansen and Nansen (1920). They attempted to account for climatological variations in the Northern Hemisphere by examining temperature

variations in the North Atlantic Ocean. Understandably, their work did not yield the answers they had hoped to find. Lack of adequate records and slow, unwieldy data processing methods hampered their work. Meteorology and oceanography were still in their infancy and consequently their biggest roadblock was the lack of understanding of the circulation in both the atmosphere and the oceans.

The problem was left virtually untouched until Jacobs (1951) examined some of the ramifications of energy exchanges between the atmosphere and the oceans. More recently, considerable attention has been focussed on the problem. The list of accomplishments is too long to be summarized and it will suffice to single out some of the most interesting recent papers by two workers actively engaged in this field.

Drought in the Northeastern United States during the period 1962-65 was accounted for by Namias (1966). The mechanism proposed was the interaction of anomalously cold water along the Continental Shelf with the overlying atmosphere.

Bjerknes (1969) established a connection between equatorial sea surface temperatures in the central Pacific Ocean, and the strength of the extratropical westerlies. He was able to demonstrate that the amount of equatorial rainfall is highly dependent upon sea surface temperatures. Variations in the amount of rainfall lead to variations in the amount of heat of condensation released, which in turn lead to fluctuations in the strength of the Hadley cell. The strength of the subtropical high, formed by subsidence of air on the northern edge of the cell, in turn depends on the strength of the Hadley cell. Since the Hadley cell transports angular momentum

northward, any variations in its strength affect the efficiency of transport and hence the strength of the extratropical westerlies.

The problem of teleconnection was attacked from a longitudinal point of view by Namias (1969). He showed that the anomalously warm sea surface temperature regime that existed over one-third to one-half of the North Pacific from the fall of 1961 to the winter of 1967-68 led to more severe winters over the eastern two-thirds of the United States. Because a major portion of this thesis deals with the effect of this anomalous sea-surface temperature regime on hail damage in Alberta, the initiation and magnitude of the anomaly will be described.

1.3 Initiation of the Anomalous Regime

Namias showed that in the fall of 1961, an anomalously strong North Pacific high developed, centred near one hundred and thirty-five degrees west longitude and thirty-five degrees north latitude. Departures from normal sea level pressure were in excess of two standard deviations. This pressure system was responsible for the warming of much of the North Pacific sea surface as a result of three cooperating factors. First, the location and intensity of the high were favourable for Ekman layer advection[1] of warm water from the south. Secondly, persistent warm and moist air advection from

---

[1] In the Northern Hemisphere, wind stresses on the surface of the ocean set up a mean transport at right angles to the wind direction (von Arx, 1962). Therefore, the circulation to the south and west of the high resulted in the northward transport of warm surface water.

the south prevented normal seasonal cooling by loss of heat from the water to cooler overlying airmasses. Thirdly, the lack of cyclonic activity resulted in considerably less wind stirring of the surface layers than normal, allowing this stable regime of warm water over cold to build.

The development of the anomalously strong high pressure system is attributed by Namias to the development of a very extensive cold pool of water over the east-central Pacific during the winter of 1960-61. The cold pool persisted through the summer of 1961 and caused low level cooling of airmasses in the fall of 1961. The resulting vertical stabilization of the atmosphere allowed the formation of a high strong enough to dominate over the Aleutian low, causing the latter to be displaced northward.

1.4 Magnitude of the Anomaly

Averaged over the period 1961-67, the sea surface temperature anomaly had a maximum value slightly in excess of two Fahrenheit degrees near thirty-five degrees north latitude and one hundred and sixty-five degrees west longitude. For the summers of this period, the highest average anomaly was not as marked, but had a value slightly in excess of 1.5 Fahrenheit degrees. The size of the anomaly hardly seems significant, but when one considers its areal extent (one-third to one-half of the North Pacific ocean), it represents a very large additional input of energy into the 'atmospheric engine'.

1.5 Objective of this Study

The aim of this study is to investigate correlations between the North Pacific sea-surface temperature anomaly and hail damage in Alberta. To accomplish this purpose, thirty-three years of hail insurance data were analyzed. Using monthly mean upper air data, the effect on the upper air circulation over Alberta are researched. Once the hail data and upper air structure have been analyzed, attempts at correlation between the circulation aloft and hail damage are possible. Correlations between precipitation and hail damage are also examined.

CHAPTER 2

THE HAIL INSURANCE DATA

2.1 The Dominion Lands Survey System

Since the hail insurance data are organized by township, a brief description of the Dominion Lands Survey System as it applies to Alberta is in order. One hundred and ten and one hundred and fourteen degrees west longitude were designated the fourth and fifth meridians, respectively. Beginning at the 49th parallel and a meridian, the land is broken up into six mile square townships (Fig. 2-1). The townships are numbered northward from the 49th parallel, and the range of a township is numbered westward from the meridians. The convergence of the meridians necessitated 'jogs' and these were allowed between townships 2 and 3, 6 and 7, and so on.

2.2 Terminology

In the jargon of the insurance business, the risk is the amount for which a given item is insured, and the loss is the amount paid out as a result of a claim. The loss to risk ratio in per cent is the loss divided by the risk, and then multiplied by 100. Quoting the loss to risk ratio in per cent is common practice and will, therefore, be followed in this thesis.

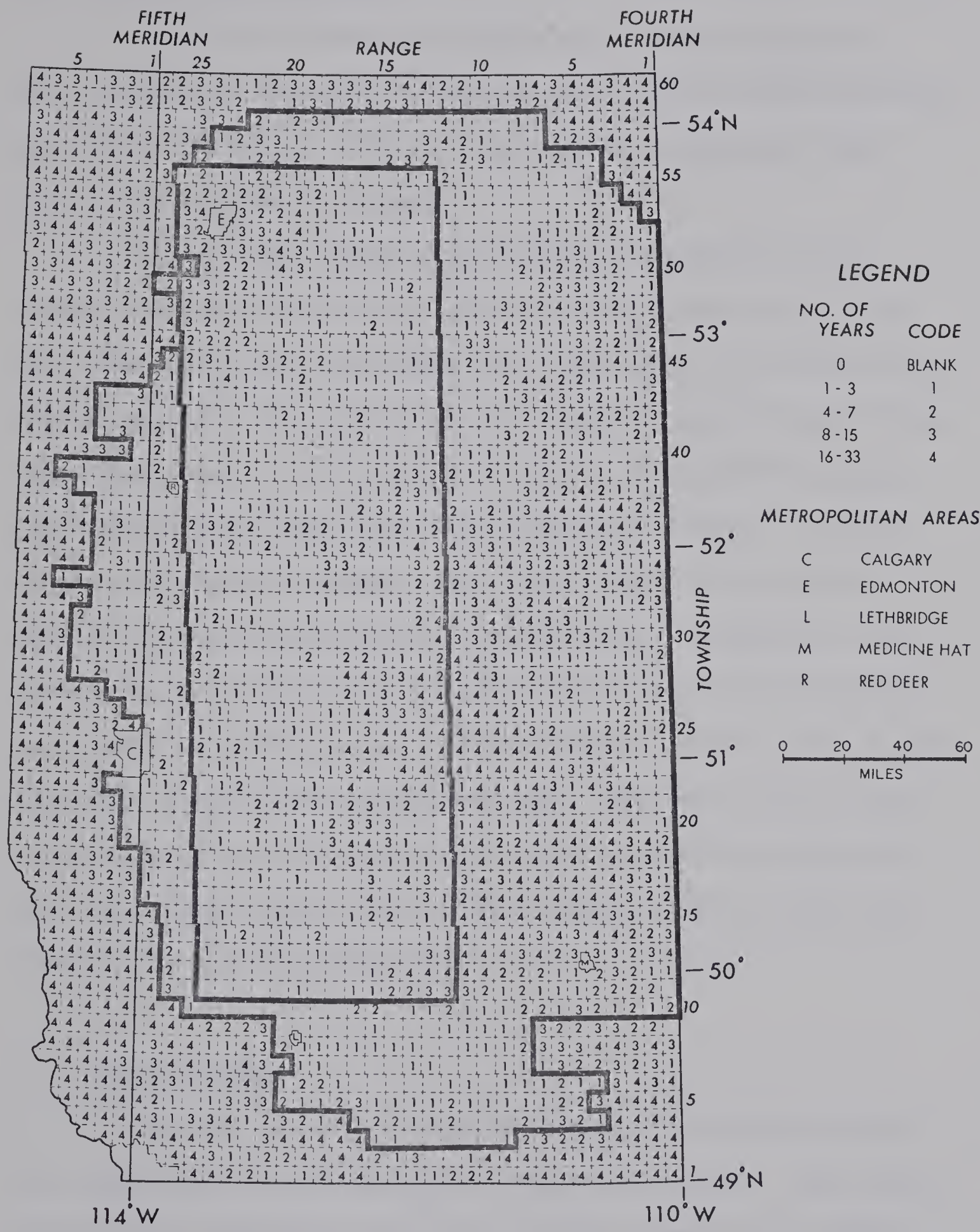

Fig. 2-1 Land divisions in Southern Alberta and the completeness of the hail insurance coverage. The code figure in each township represents the number of years for which no insurance was taken out. The two analysis areas are outlined by heavy black lines.

2.3 The Hail Insurance Data

In 1970, the Alberta Hail and Crop Insurance Corporation made available on microfilm to Alberta Hail Studies its hail insurance records for the period 1938-70. These records contain the total annual risk and loss by township.

Alberta Hail Studies staff extracted the risk and loss figures and entered them in a log to the nearest ten dollars. The data were then punched onto eight track paper tape and transferred to Digital Equipment Corporation ten track magnetic tapes using the fast paper tape reader on the Research Council of Alberta PDP-9 computer. The risk and loss figures were then checked by comparing a printout of the data stored on magnetic tape with the microfilm records. Most of the errors were detected in this manner. Comparison of the sums of the risks and losses for each township for the thirty-three year period as calculated on the PDP-9 computer, with the sums on the microfilm, revealed some inconsistencies. These were resolved after correspondence with the Alberta Hail and Crop Insurance Corporation. This task, which yielded five ten track magnetic tapes of data, was completed by early September 1971.

2.4 Analysis Areas

In order to establish the boundaries of the analysis area, the completeness of the insurance coverage was examined. The results are shown in coded form in Fig. 2-1. In each township, the figure plotted represents the number of years for which no hail insurance was taken out. If insurance was taken out for every year of the

thirty-three year period in a given township, that township was left blank.

Two analysis areas were chosen. The first is the quasi-rectangular area shown in Fig. 2-1. It is bounded by the southern and northern edges of townships eleven and forty-five (in the south and north), respectively, and by the eastern and western edges of ranges thirteen and twenty-six, respectively (in the east and west). This area, which will be referred to as the small area, covers 22,680 square miles. The second and larger area is outlined by the irregular heavy line. This area, which will be referred to as the large area, covers approximately 52,000 square miles.

The western boundary of the large analysis area demarcates (for all intents and purposes) the western extreme of cultivated land in southern Alberta. To the west of this boundary are forested areas and the foothills of the Rockies. In an attempt to include as much of the data as possible, some areas with very little or no insurance coverage were included in the large analysis area. The area that stands out most is to the north-north-west of Medicine Hat, which includes the Suffield Defence Research Establishment and the dry lands in the vicinity of Hanna.

It should be noted that for those areas of the province which are under cultivation and for which no insurance was taken out for fifteen years or less, most of these years are prior to 1950. This is probably because of the trend toward larger farms, increasing mechanization and crop values, and popularity of the hail insurance program. The increase in risk is shown in Fig. 2-2 which shows the total risk written in the large analysis area versus time.

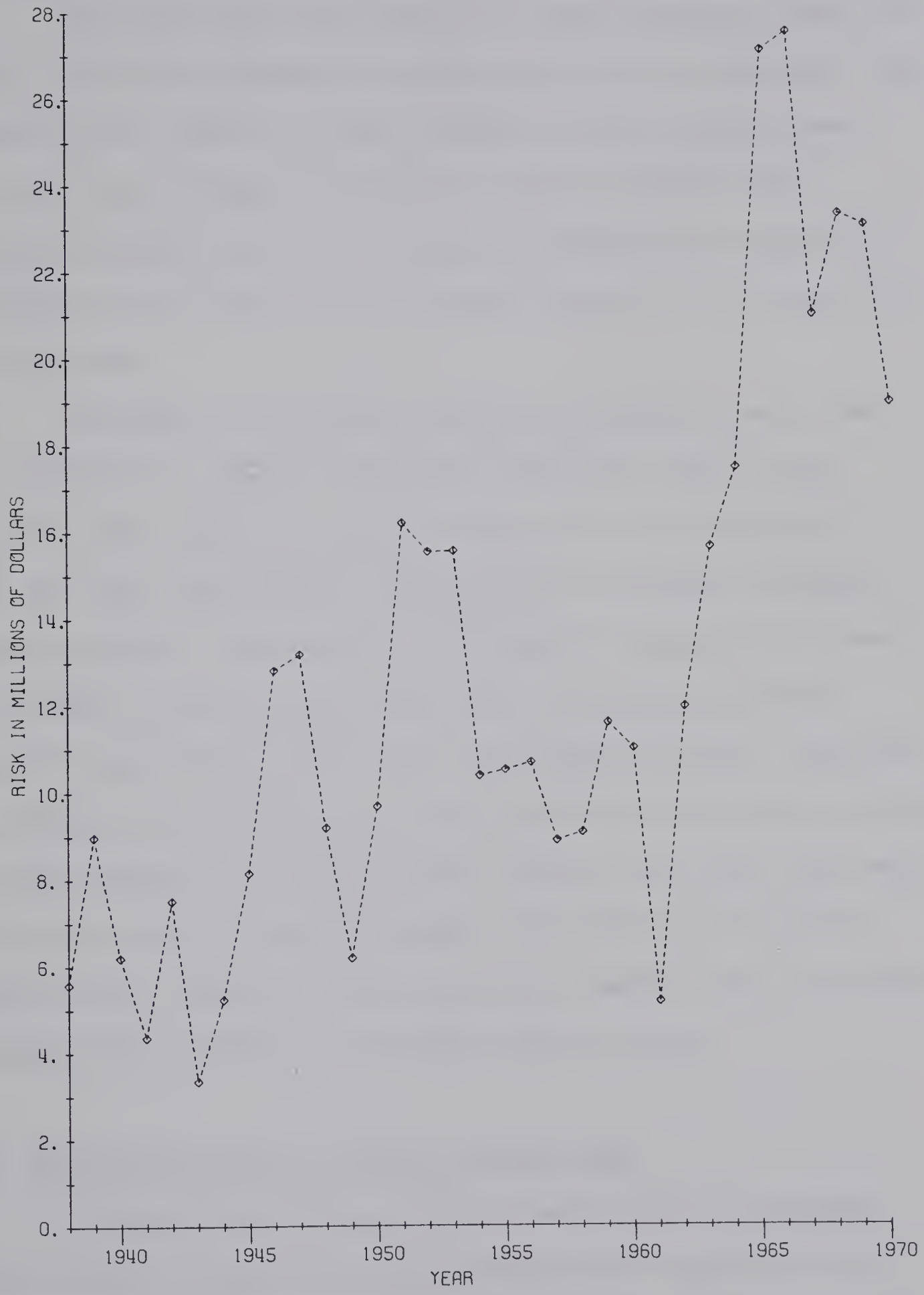

Fig. 2-2 Amount of risk written annually in the large analysis area during the period 1933-70.

2.5 Reduction of the Data

The first step in the analysis of the data was to reduce its volume. This was performed by summing separately the risks and losses across all the ranges of a given township for each analysis area. This task was performed on the Alberta Research Council PDP-9 computer, yielding two 33 x 45 arrays for the small area (years vs. townships; one for risks, one for losses) and two 33 x 56 arrays for the large area.

The amount of storage available on the PDP-9 computer was not sufficient to perform calculations using such large arrays. Therefore, the reduced data had to be put into a form compatible with the I.B.M. Model 360-67 computer at the University of Alberta Computing Centre. Unfortunately, the ten-track magnetic tapes used on the PDP-9 cannot be read on the I.B.M. seven and nine track magnetic tape drives on the I.B.M. Model 360-67 computer. Therefore, the reduced data were printed out using the PDP-9 line printer facility, and then punched onto standard eighty column I.B.M. punch cards using the I.B.M. model 029 keypunch machine. The data were then listed using an I.B.M. model 1403 line printer and compared with the listings produced using the PDP-9 to eliminate punching errors.

2.6 Time Series Analysis of Hail Insurance Data

Attempts to determine trends in hail damage by examining plots of loss to risk ratio versus time for each township were not very fruitful. To obtain an overall view, the losses and risks for individual townships were summed separately for each year for both

analysis areas. From these totals, the average annual loss to risk ratios were obtained. The resulting time series are shown in Figs. 2-3 A and B. Because of the very large variation in the average loss to risk ratio, the time series was smoothed using the seven point approximation to a Gaussian filter given in Table 2-1. The subscript for a given weighting factor indicates the year to which that factor is applied.

Table 2-1 Weights for seven point Gaussian filter (Holloway, 1958).

W_{t-3}	.016
W_{t-2}	.094
W_{t-1}	.234
W_t	.312
W_{t+1}	.234
W_{t+2}	.094
W_{t+3}	.016

This filter was chosen rather than the running mean, which is commonly used in meteorology, because it lacks the undesirable frequency response characteristic of the latter.

The smoothed time series for both areas show maxima centred at about 1945, followed by minima in 1949. The loss to risk ratios increased again to maxima in 1953, followed by a slow decrease. In the early sixties, the decrease becomes more marked. In fact, the

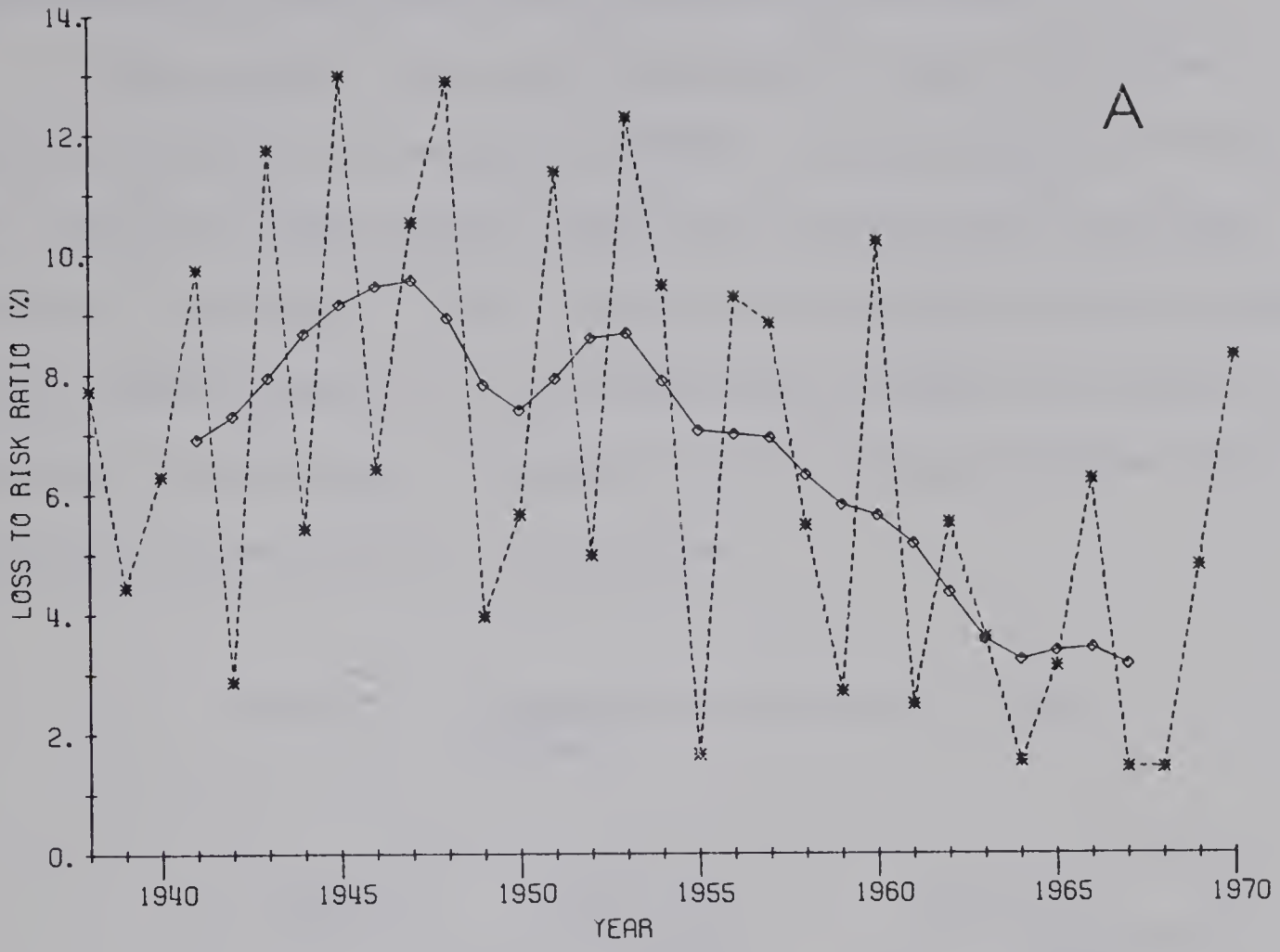

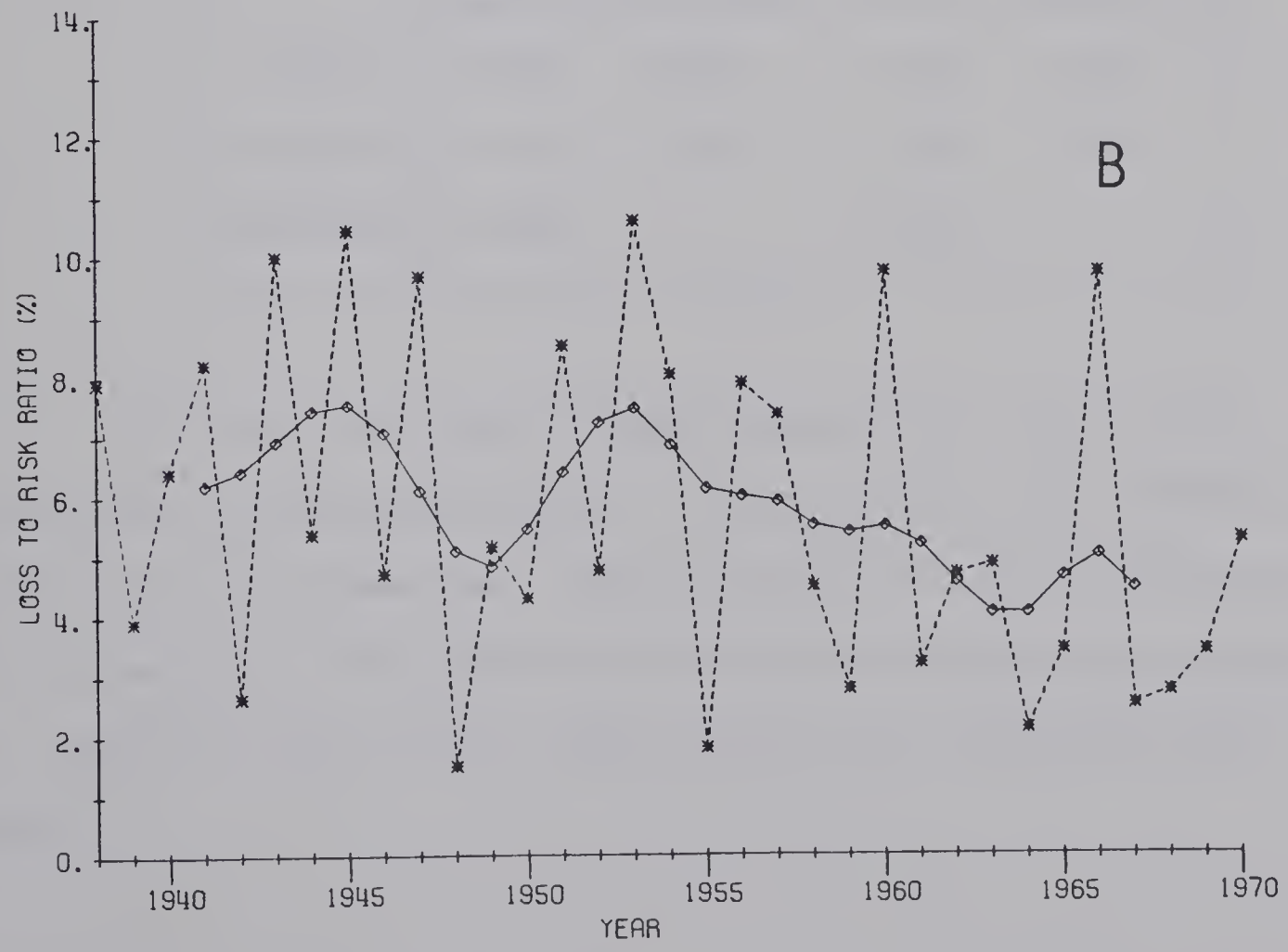

Fig. 2-3 Variation of loss to risk ratio for period 1938-70 for small area (A) and large area (B). Asterisks represent actual annual loss to risk ratios, and diamonds the smoothed values.

smoothed series reach their lowest points at this time.

The anomalous sea surface temperature regime lasted from the fall of 1961 to the winter of 1967-68. From the point of view of hail production, the anomalous period was therefore from the summer of 1962 to the summer of 1967. Comparing the twenty-four years prior to the anomalous period with the period itself reveals the extent of reduction of hail damage. Table 2-2 has the mean and standard deviations for the two periods for both areas.

Table 2-2 Comparison of mean loss to risk ratios.

PERIOD	LARGE AREA		SMALL AREA	
	Mean	Standard Deviation	Mean	Standard Deviation
1938-61	6.23%	2.87%	7.01%	3.59%
1962-67	4.55%	2.78%	3.59%	2.00%
REDUCTION	1.68%		3.42%	

Both areas show quite a marked reduction in loss to risk ratio during the anomalous period. In the small area, the reduction is by a factor of almost two. Listed in Table 2-3 are the mean loss to risk ratios for both areas for six year periods beginning in 1938. The reduction is seen to be a unique event in the thirty-three year period.

Table 2-3 Mean loss to risk ratios for six year periods.

PERIOD	LARGE AREA	SMALL AREA
1938-43	6.52%	7.10%
1944-49	6.14%	6.78%
1950-55	6.34%	7.60%
1956-61	5.92%	6.53%
1962-67	4.55%	3.59%

A long-term downward trend in the loss to risk ratios can be seen as well. The change toward larger, more economically viable farms may be responsible for this trend. The resultant increased insurance coverage into areas less susceptible to hail damage can account for the gradual reduction in the loss to risk ratios in the two analysis areas. Summers (1966) mentions other possible causes. Changes to crops more resistant to hail damage may be responsible for the decrease. Long term climatic changes may have occurred as a result of a change in the large-scale weather pattern in Western Canada or the changes brought about by man's increased interference in nature by farming, forestry, mining and manufacturing. The amount of risk written could possibly influence the loss to risk ratio as well.

However, it can be stated that at the time of the anomalous sea-surface temperature regime, a marked reduction in hail damage in Alberta occurred. Significance testing of the data is not possible. The condition that the distribution of loss to risk ratios be normal is not met, as indicated by Table 2-4.

Table 2-4 Frequency distributions of loss to risk ratios for large and small areas.

CLASS	LARGE AREA FREQUENCY	SMALL AREA FREQUENCY
0.00-0.95%	0	0
1.00-1.95%	2	5
2.00-2.95%	5	3
3.00-3.95%	4	3
4.00-4.95%	6	2
5.00-5.95%	3	5
6.00-6.95%	1	3
7.00-7.95%	3	1
8.00-8.95%	3	2
9.00-9.95%	3	3
10.00-10.95%	3	2
11.00-11.95%	0	2
12.00-12.95%	0	1
13.00-13.95%	0	1

2.7 Shift in Hail Damage

To determine if any latitudinal shift in hail damage occurred during the anomalous period, the large analysis area was divided into six latitudinal strips, each nine townships wide. For each strip, the average annual loss to risk ratio was determined. The resulting time series were smoothed using the Gaussian filter. The resulting series shown in Fig. 2-4 plotted on a common time axis, show that quite marked north-south variations did occur. From the point of view of teleconnection, the most significant feature is the high loss to risk ratio for townships four to twelve. This strip is the only one for which the loss to risk ratio is above normal for the period 1962-67, suggesting that a southward shift in hail damage may have occurred. Confirmation of this shift would require examination of the hail insurance records for Montana.

2.8 Correlation Between Annual Loss to Risk Ratio and Precipitation

Many farmers of Alberta consider a wet spring a harbinger of heavy hail damage in the summer. Using hail insurance and precipitation data, this commonly held belief was investigated.

In February of 1972, Alberta Hail Studies transferred the hail insurance data from ten track to nine track magnetic tape, permitting the computation of loss to risk ratios by river basin. Monthly mean precipitation for the Red Deer, North Saskatchewan, and South Saskatchewan river basins were used to attempt a correlation between precipitation and the annual loss to risk ratios. The coefficient calculated is using the formula:

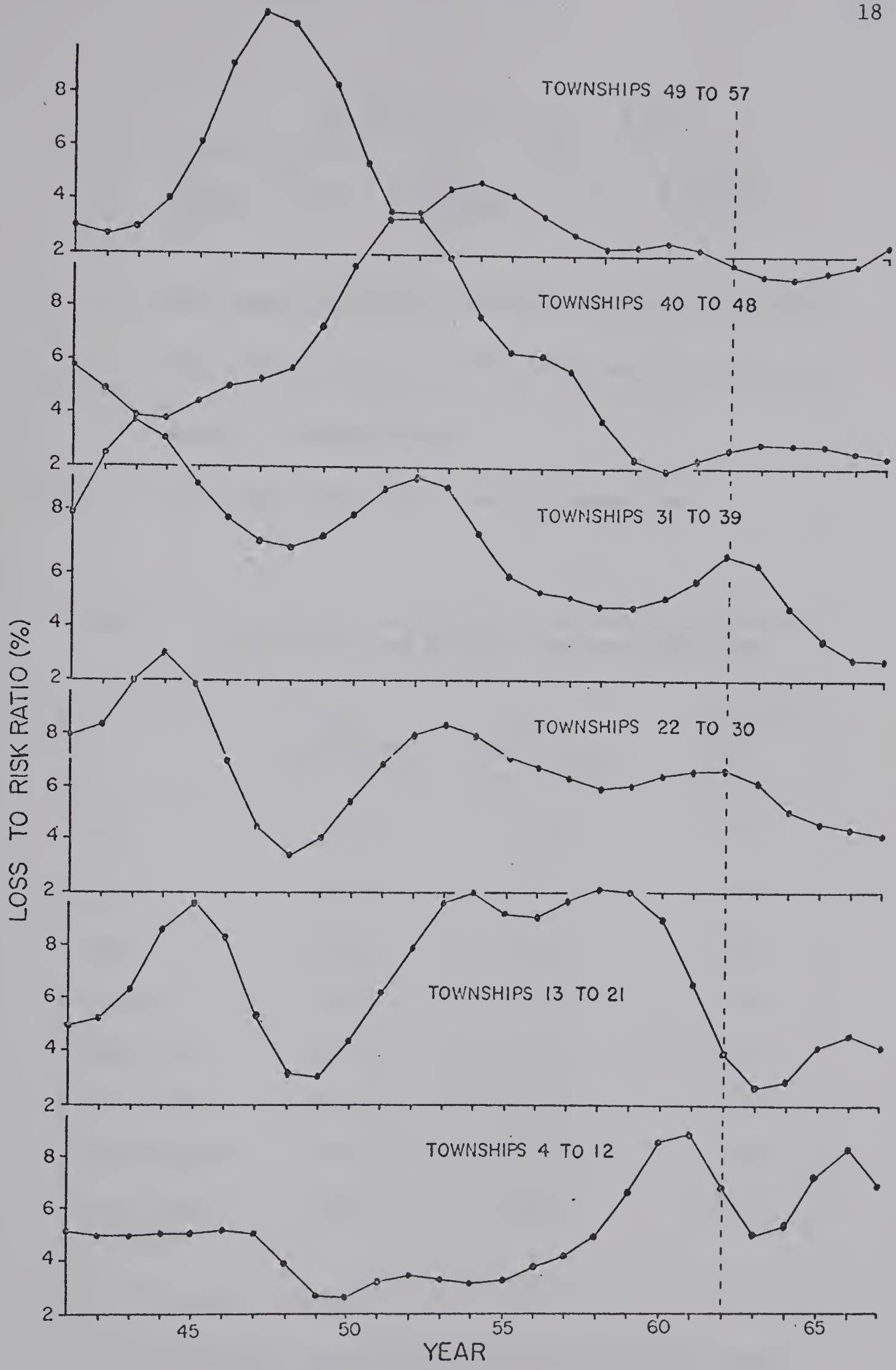

Fig. 2-4 Smoothed time series of loss to risk ratio for six strips, each nine townships wide, in the large analysis area.

$$r_{jk} = \frac{\frac{1}{N}\sum_{1}^{N}\left[(X_j - \bar{X}_j)(X_k - \bar{X}_k)\right]}{\left\{\left[\frac{1}{(N-1)}\sum_{1}^{N}(X_j - \bar{X}_j)^2\right]\left[\frac{1}{(N-1)}\sum_{1}^{N}(X_k - \bar{X}_k)^2\right]\right\}^{1/2}}$$

r_{jk} = the sample correlation coefficient between X_j and X_k

X_j, X_k = the variates (loss to risk ratios and precipitation)

N = number of observations

$\bar{X}_j$, $\bar{X}_k$ = the sample means of X_j and X_k respectively

Table 2-5 Correlation coefficients between annual loss to risk ratios and monthly mean precipitation.

	South Saskatchewan River Basin	North Saskatchewan River Basin	Red Deer River Basin
May	-0.249	-0.180	0.095
June	-0.099	-0.034	0.079
July	-0.026	0.101	-0.048
August	0.480	0.107	0.444
May+June	-0.206	-0.111	0.113
June+July	-0.103	0.034	0.038
July+August	0.372	0.164	0.330
June+July+ August	0.171	0.097	0.327

The correlation coefficients obtained certainly do not support the belief that heavy spring rainfall is followed by heavy hail damage in the summer. If anything, the negative coefficients

for the North and South Saskatchewan River basins for May indicate that the converse may be true.

The highest correlation coefficients obtained are for August in the Red Deer and South Saskatchewan River basins. This is hardly surprising. August precipitation is largely due to convective activity, rather than frontal or cold low weather systems. The storms which produce hail are also the ones which supply much of the August rainfall.

The results imply that the low level advection of moisture which occurs in the typical severe storm situation is the major source of moisture for the storms. Water vapour flux from the soil to the overlying airmass by means of evaporation or transpiration is of secondary importance.

CHAPTER 3

THE OBJECTIVE ANALYSIS

3.1 Introduction

To examine the relation between the hail damage and the mean upper wind fields, analyses of the monthly mean upper air data were required. These are available in the Monthly Weather Review up to 1952 and in the National Summary of Climatological Data of the U.S. Weather Bureau from 1953. However, since interpolation on these maps, which are contoured at intervals of sixty gpm., is not very satisfactory, it was decided to analyze the monthly mean data for the levels of interest using an objective technique.

3.2 Analysis Area

The analysis was performed on the 8 x 9 grid, shown in Fig. 3-1, which has the 381 km gridlength used at the National Meteorological Centre of the United States Weather Bureau (referred to hereafter as N.M.C.). The grid is oriented parallel to 110° west longitude instead of 80° west longitude for the standard N.M.C. grid. The analysis area contains twenty-three upper air sounding stations. The records were complete for the period 1950-70 with the following exceptions:

Fig. 3-1 The objective analysis grid and upper air stations used in the analysis.

Upper Air Station	Years for which data available
Annette, Alas.	1955-70
Coppermine, N.W.T.	1950-69
Salem, Oreg.	1956-70
Tatoosh Island, Wash.	1950-66
Quillayute, Wash.	1967-70

3.3 Data

The data used in the analyses are the 700, 500, 400, 300, and 200 mb monthly mean geopotential heights and the vector mean winds (when available) for the months July and August. They were extracted from the following sources:

Canadian Data	Period
Summaries of Radiosonde Observations in Canada	1950-58
Monthly Bulletin of Canadian Upper Air Data	1959-70
U.S. Data	
Monthly Weather Review	1950-52
Climatological Data, National Summary	1953-70

Prior to the conversion to radio direction finding radiosondes, only the monthly mean geopotential heights were available. This conversion took place in 1956 in the U.S.A. and in 1959 in Canada.

After extraction, the data were punched onto I.B.M. cards using an I.B.M. Model 029 keypunch machine. The data were then listed, using

an I.B.M. Model 1403 line printer to facilitate easier checking of the punched data. A few errors which escaped detection at this point were subsequently caught during the execution of the objective analysis, which rejects data that do not fall within specified error limits.

The reason for examining the mean wind fields for July and August only can be readily seen upon examination of Fig. 3-2, which shows the seasonal variation of the total number of hail damage claims in Alberta for the period 1946-66 (after Summers and Paul, 1967). The bulk of the claims were made for storms occurring in July and August. Damaging storms do occur in June and September, but their frequency is low compared with July and August, and they occur before insurance is taken out, or after a large proportion of the crops has been harvested.

3.4 Analysis Method

The analysis method used is basically that described by Cressman (1959) and used by N.M.C. The program used was that of Linton et al. (1971), which is essentially a revised and improved version of the Glahn and Hollenbach (1959) program.

The method is one of successive approximations to the height using the geostrophic wind-height relationship whenever possible to modify the first guess. The analysis is performed in a series of five passes over the data field. On each pass, an observation (height, wind speed, and wind direction) results in an adjustment to the height at all gridpoints within a distance of R gridlengths, where R is the radius of influence. R is large for the first pass and is decreased on later passes to a minimum of two gridlengths on the fifth

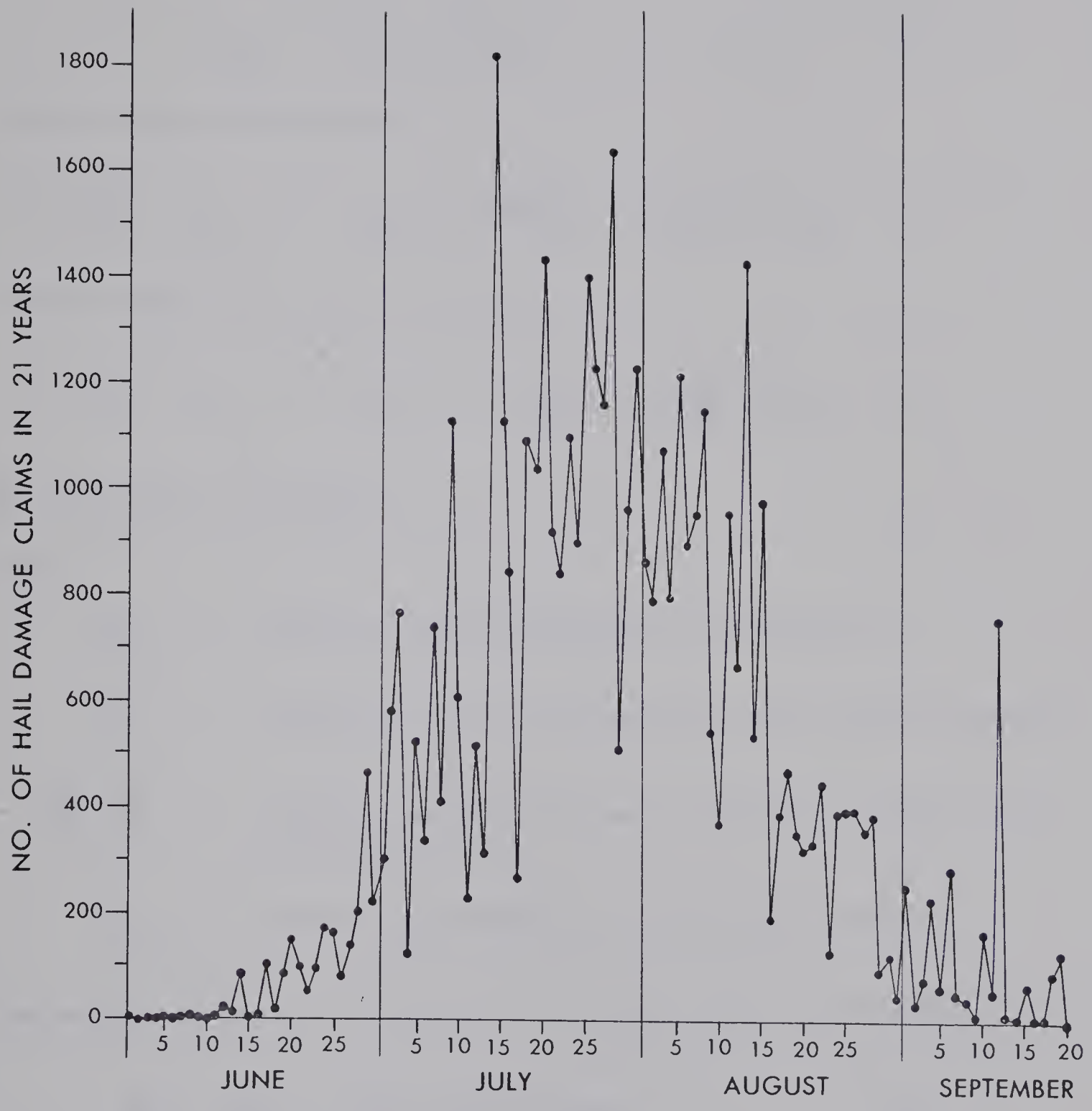

Fig. 3-2 Seasonal variation of the total number of hail damage claims in Alberta during the period 1946-66. (after Summers and Paul, 1967)

pass.

For each observation, one of the three following correction terms is computed:

$$\text{(i)} \qquad C_{1_{i,j}} = (Z_{x,y} - \hat{Z}_{x,y}) \qquad 3\text{-a}$$

if only height is available

$$\text{(ii)} \qquad C_{2_{i,j}} = [Z_{x,y} + (i-x)\frac{\partial Z}{\partial y} + (j-y)\frac{\partial Z}{\partial y} - \hat{Z}_{i,j}] \qquad 3\text{-b}$$

if both height and wind are available

$$\text{(iii)} \qquad C_{3_{i,j}} = [\hat{Z}_{x,y} + (i-x)\frac{\partial Z}{\partial x} + (j-y)\frac{\partial Z}{\partial y} - \hat{Z}_{i,j}] \qquad 3\text{-c}$$

if only wind is available

where

$Z_{x,y}$ = observed height at station at position x,y

$\hat{Z}_{x,y}$ = height at station interpolated from current analysis

$\frac{\partial Z}{\partial x}, \frac{\partial Z}{\partial y}$ = height gradients in x and y directions respectively, at gridpoints i,j

$\hat{Z}_{i,j}$ = height at gridpoint i,j from current analysis

The height gradients are computed by the geostrophic relationships:

$$\frac{\partial Z}{\partial x} = \frac{fv}{g} = .782 \sin\phi\,(1+\sin\phi)v \qquad 3\text{-d}$$

$$\frac{\partial Z}{\partial y} = \frac{fu}{g} = .782 \sin\phi\,(1+\sin\phi)u \qquad 3\text{-e}$$

where

u = observed eastward wind component

v = observed northward wind component

ϕ = the latitude of the observing station

g = the acceleration due to gravity

f = the Coriolis parameter

When u and v are used in knots, $\frac{\partial Z}{\partial x}$ and $\frac{\partial Z}{\partial y}$ are in metres/grid unit at the latitude of the station.

The total correction to the height at a given gridpoint is obtained by combining the individual correction terms in one of three ways:

$$\text{(i)} \qquad C_a = \frac{1}{n} \sum_{k=1}^{n} C_{m_{i,j}} \qquad 3\text{-f}$$

$$\text{(ii)} \qquad C_b = \frac{1}{n} \sum_{k=1}^{n} \frac{[R^2-d_k^2]C_{m_{i,j}}}{R^2+d_k^2} \qquad 3\text{-g}$$

$$\text{(iii)} \qquad C_c = \frac{\frac{1}{n} \sum_{k=1}^{n} \left[\frac{R^2-d_k^2}{R^2+d_k^2}\right] C_{m_{i,j}}}{\frac{1}{n} \sum_{k=1}^{n} \frac{R^2-d_k^2}{R^2+d_k^2}} \qquad 3\text{-h}$$

where

n = number of observations within R of the gridpoint

d = the distance from the observing station to the gridpoint

m = the type of correction 1, 2, or 3, and

$C_{m_{i,j}}$ = the individual correction terms

C_b and C_c result in variable weighting of the individual corrections in a manner such that the closer a station is to a grid-point, the greater the weight of the total correction. C_a and C_c cause more rapid convergence than C_b. Hence, C_c and C_a were used on passes one and two respectively to obtain an analyzed height field which showed the major features. C_b was used on the last three passes, with successively decreasing radius of influence, to obtain the smaller features of the upper air structure.

3.5 Smoothing

Experimentation indicated that very little smoothing was required when working with monthly mean data. The smoothing operator used in the program is a modification of Cressman's (1959) operator as used by Thomasell and Welsh (1959):

$$S_{i,j} = \frac{A_{i,j} + b\bar{A}_{i,j}}{1 + b} \qquad 3\text{-}i$$

where

$S_{i,j}$ = the smoothed height at gridpoint i,j

$A_{i,j}$ = the current height at gridpoint i,j

$\bar{A}_{i,j}$ = $1/4\ (A_{i+i,j} + A_{i,j+1} + A_{i,j-1} + A_{i-1,j})$

b = smoothing parameter

The value of b used on all five passes was 0.5.

3.6 Output

The analysis was printed in a "zebra-stripe" fashion, as shown in Figs. A-1 through A-5 of Appendix A, in which the contours are the boundaries between the alternate blank and printed bands. The contour interval used was 30 gpm. Labelling was done by printing the last three figures of the height at each gridpoint using F-format in a manner such that the decimal is at the location of the gridpoint. For example, the figure 354. in the pattern produced for a 300 mb analysis indicates that the geopotential height at that gridpoint is 9354 gpm.

3.7 Testing the Program

Results of the objective analysis were compared with results of hand analyses and with maps published in the National Summary of Climatological Data. The comparison indicated that the objective analysis program produced a very good height field in the area of interest. To test the effect of the initial height field on the results of the analysis, the height field was initialized to different values. The first was a level surface close to the average value of the heights, the second to zero height (the value of the datum level), and the third to a sloping field higher in the south than in the north such that the initial "wind" blew from west to east. The results in all three cases were identical to the very last symbol in the output pattern, indicating that the initial height field had no effect on the final result and that the method is computationally stable.

Because wind data were not available for all years, a test was performed to determine the effect of missing wind data. After performing an analysis on data which included wind speed and direction, the latter were removed and the analysis was repeated. The two results were in good agreement. The removal of the wind data resulted in insignificantly lower heights over the area of interest, namely the southern half of Alberta, the average decrease being 2.5 gpm. The gradients and their directions differed by no more than six gpm per grid interval and eight degrees.

Shown in Figs. A-1 through A-5 of Appendix A are five examples of the output of the objective analysis program, one for each level. To facilitate interpretation, the output was photographed after being overlaid with an acetate showing the coastal outlines, provincial, state, and federal boundaries, major bodies of water, and the upper air stations used in the analysis.

CHAPTER 4

ANALYSIS OF THE CIRCULATION

4.1 Introduction

It is difficult to interpret an effect of the anomalous sea-surface temperature regime in the North Pacific on the circulation over Alberta from the isobaric charts for the five levels analyzed. Consequently, meridional-vertical cross-sections through the atmosphere were constructed.

It was possible to overcome the lack of wind data for the period prior to the conversion to radio direction finding radiosondes by using the height fields produced by the objective analysis and the geostrophic wind-height relationship. In order to avoid the problems of attempting to compare observed winds for the period 1959-70 with calculated winds for the period 1950-58, it was decided to use the geostrophic wind equation to calculate winds for the entire period. This method has the added advantage of increasing the number of data points. Using observed wind data to draw cross-sections would allow one to use five data points, namely, the observations for Lander, Great Falls, Edmonton, Fort Smith, and Coppermine. Calculated winds at grid centres yield eight points over the same distance, facilitating the drawing of isotachs (lines of constant wind speed) and isogons (lines of constant wind direction).

4.2 Calculation of the Winds

The monthly mean winds were calculated using the geostrophic wind equation:

$$u = -\frac{g}{f}\frac{\partial Z}{\partial y} \qquad 4\text{-a}$$

$$v = \frac{g}{f}\frac{\partial Z}{\partial x} \qquad 4\text{-b}$$

and

$$V = (u^2+v^2)^{1/2} \qquad 4\text{-c}$$

$$\theta = 270 - \arctan(u/v) \qquad 4\text{-d}$$

where

u = the eastward wind component

v = the northward wind component

V = the wind speed

θ = the wind direction (degrees)

f = the Coriolis parameter

Z = the geopotential height

g = the acceleration due to gravity

In finite difference form and in map coordinates the component equations become,

$$u_i = -\frac{gm}{fd}\left(Z_{i,j} - Z_{i+1,j} + Z_{i,j+1} - Z_{i+1,j+1}\right) \qquad 4\text{-e}$$

$$v_i = \frac{gm}{fd}\left(Z_{i,j+1} - Z_{i,j} + Z_{i+1,j+1} - Z_{i+1,j}\right) \qquad 4\text{-f}$$

where

m = $1.866/(1+\sin\phi)$ is the map factor for a polar stereographic projection, secant at 60 degrees north latitude

ϕ = the latitude angle

d = 381 km, is the grid interval

$Z_{i,j}$ = the geopotential height at gridpoint i,j

The heights for columns four and five of the objective analysis output were used to obtain winds at the grid centres. Hence subscript j has the value four, and i ranges from one to eight. This gave a quasi-meridional cross-section, one-half gridlength west of 110 degrees west longitude, and extending from approximately 43 to 67.5 degrees north latitude. The u and v components, wind speed, and wind direction were output in punched form for later use.

4.3 Construction of the Cross-sections

The punched output described above was used as data for a program that plotted the numerical data on a cross-section form using a Calcomp plotter. The wind speed and direction at each grid centre and each level for July or August was plotted for each of the twenty-one years for which the objective analysis was performed. Isotachs and isogons were drawn by hand, the former in intervals of two metres per second, and the latter in intervals of ten degrees. The results are shown in Fig. B-1 through B-21 of Appendix B.

Examination of the cross-sections reveals a marked change in the circulation over Alberta during the period 1962-67. The extent of the change is pointed out by the averaged cross-sections.

4.4 Averaged Cross-sections

The vector mean wind at each grid centre was determined for the periods 1950-61 and 1962-67. The results were then plotted and analyzed as for the monthly mean cross-sections. Examination of the averaged cross-sections reveals that, for both July and August for the period 1962-67 (Figs. 4-2 and 4-4 respectively), the strength of the mean jet was greater than for July and August for the period 1950-61 (Figs. 4-1 and 4-3 respectively), and that it had shifted southward. The extent of the southward shift was at least one grid-length or approximately 381 km. A more precise estimate is not possible from this analysis because the cross-sections do not extend south far enough. The average increase in the jet maximum was approximately 11 ms^{-1} for July and 7 ms^{-1} for August. The jet stream structure during the anomalous period is also characterized by much stronger horizontal wind shears on the north side of the jet. After 1967, the upper wind structure reverted to a pattern more like that prior to 1962 as seen in Figs. B-19 through B-21 of Appendix B.

4.5 Stratification of the Data

In order to obtain a correlation between the mean wind structure as shown on the monthly mean cross-sections and hail damage, the hail data was stratified for the period 1950-70. On the basis of the annual loss to risk ratios for the small and large analysis areas, the years in the period 1950-70 were classified as high, intermediate, or low hail damage years. For a given year to be designated as high, the loss to risk ratio had to be in the highest seven years for both the large and small analysis areas, and similarly

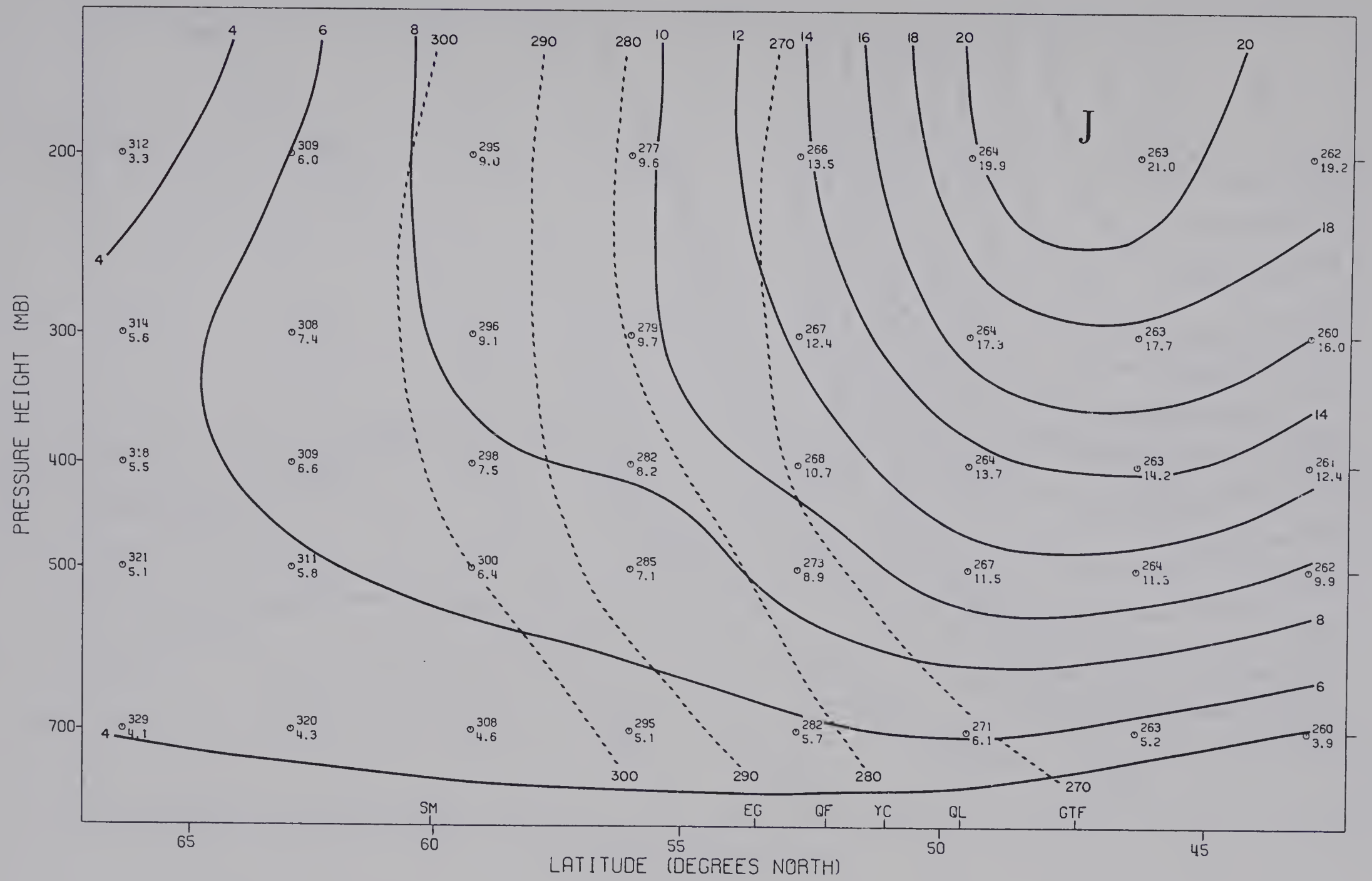

Fig. 4-1 Averaged cross-section for July for the period 1950-61.

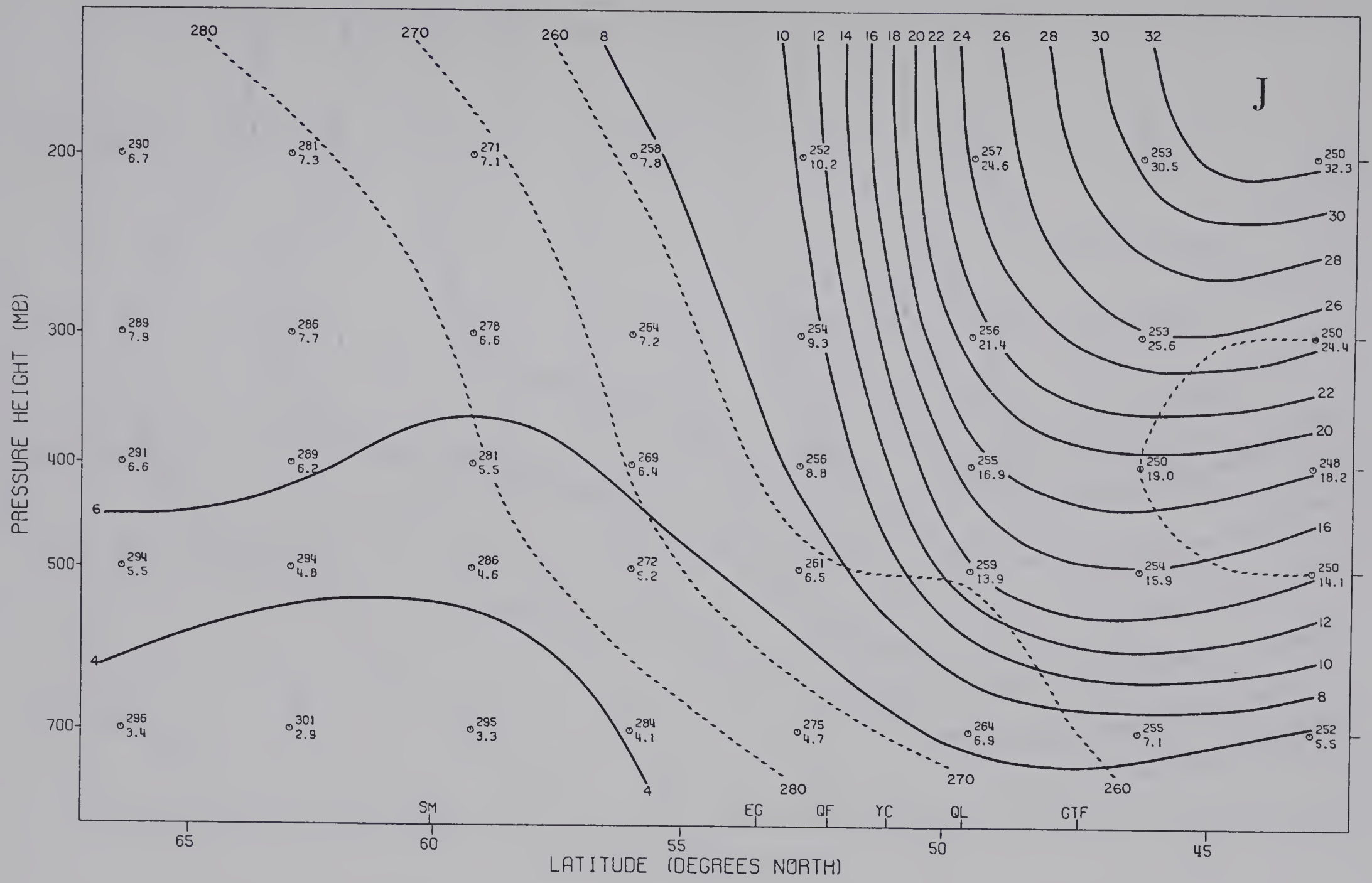

Fig. 4-2 Averaged cross-section for July for the period 1962-67.

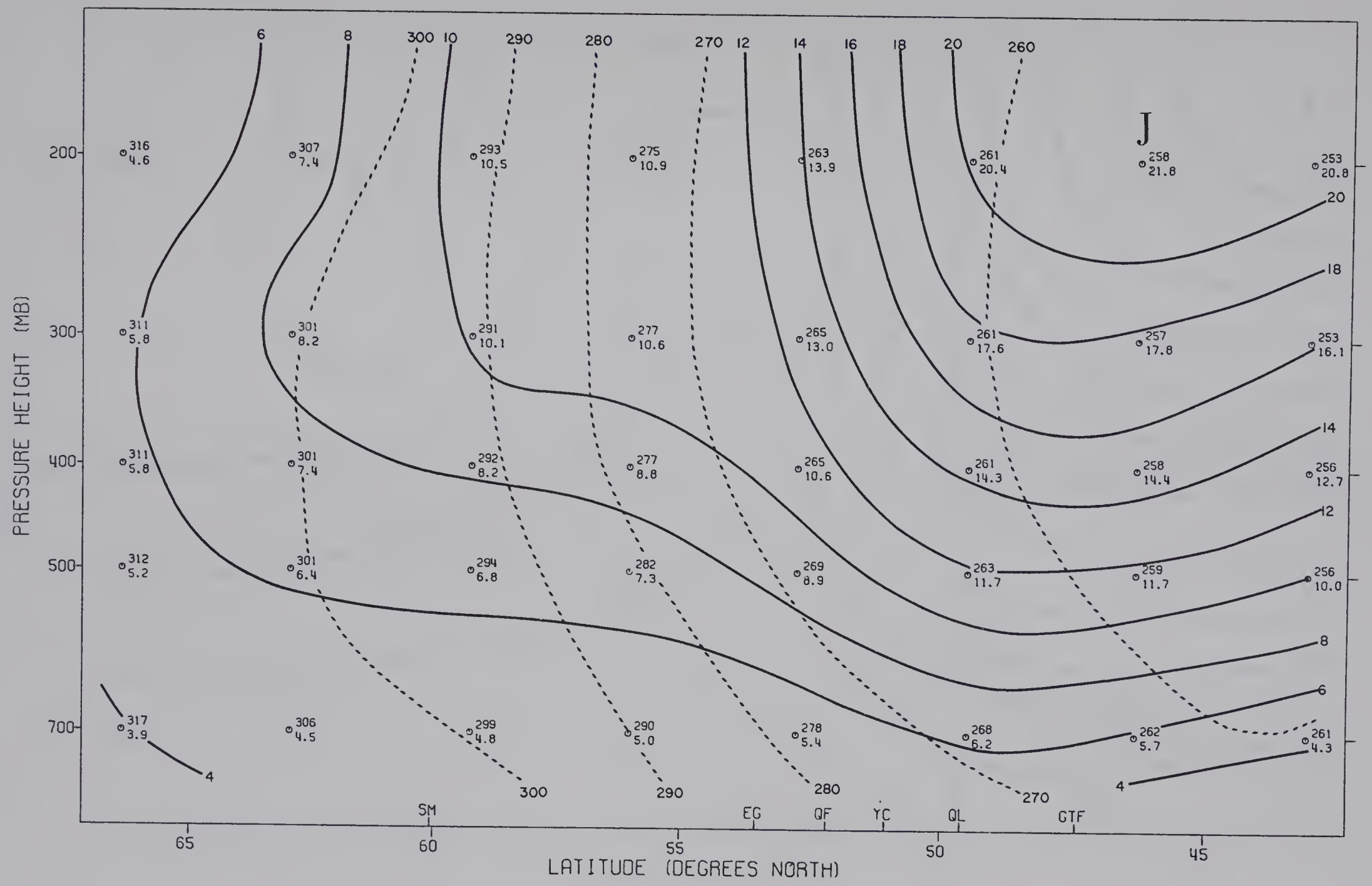

Fig. 4-3 Averaged cross-section for August for the period 1950-61.

Fig. 4-4 Averaged cross-section for August for the period 1962-67.

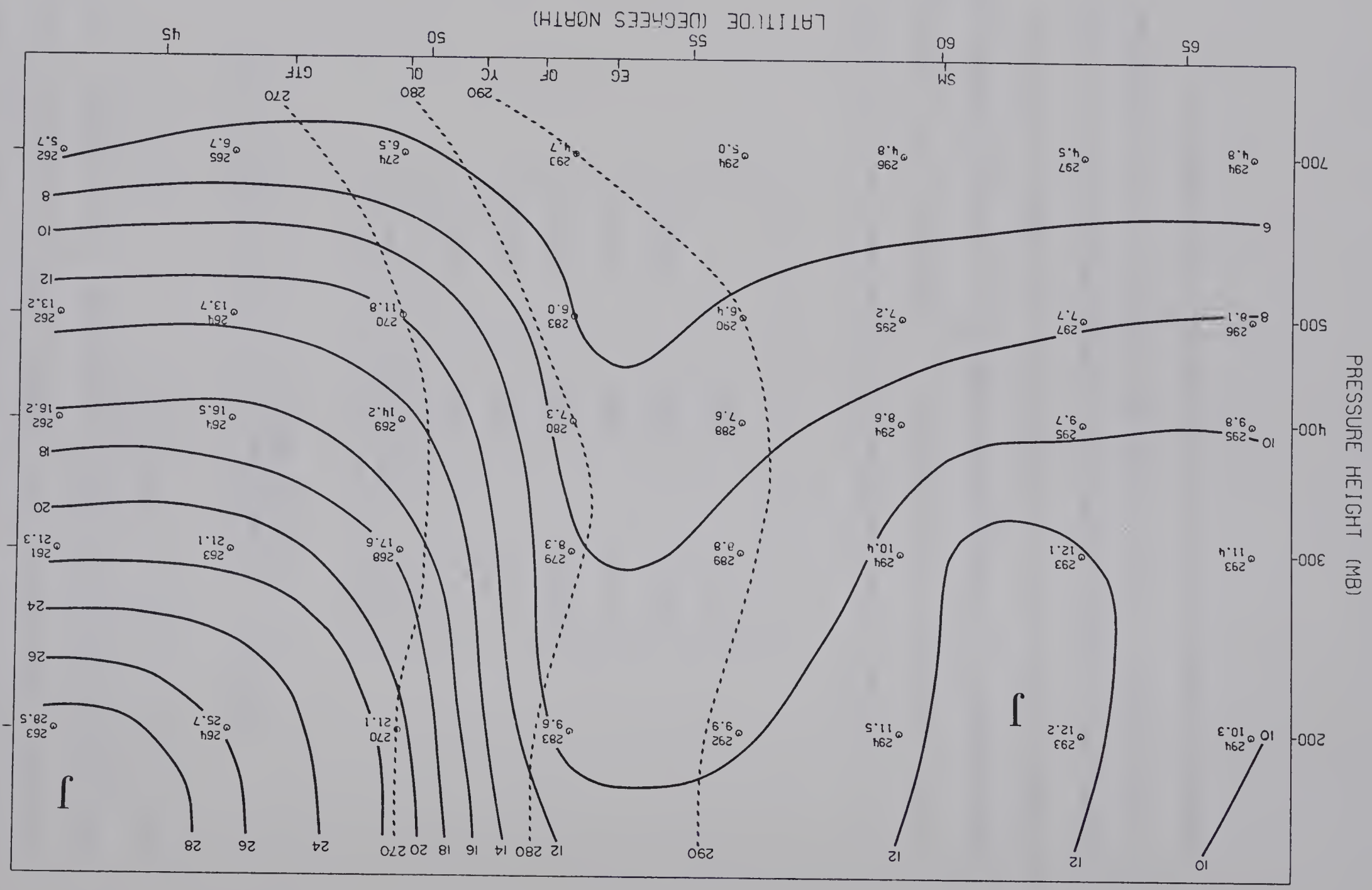

for the other categories. The year 1970 failed to meet this last criterion. Three years (1961, 1963, and 1965) for which the loss to risk ratio was borderline, were not included in the analysis. The stratification is shown in Table 4-1.

Table 4-1 Stratification of data according to loss to risk ratio.

High	Intermediate	Low
1951	1950	1955
1953	1952	1959
1954	1958	1964
1956	1962	1967
1957	1966	1968
1960	1969	

The mean cross-sections for each category were calculated for July and August as in section 4.4. Inspection of the resulting cross-sections for position of the mean jet stream and the mean wind strength or shear over the analysis area (approximately 49 to 54 degrees north latitude) revealed no common denominator for a given loss to risk category. In fact, there was little consistent difference between the cross-sections for the low and high categories.

4.6 Correlation Between Yearly Loss to Risk Ratios and Other Meteorological Parameters

In an attempt to ascertain whether certain meteorological parameters or combination of parameters were favourable for the production of high hail damage, various scatter diagrams were produced. Plots of loss to risk ratio versus monthly mean 300 mb wind speed failed to show any correlation. Similarly, three way scatter diagrams, with monthly mean 300 mb wind direction versus monthly mean 300 mb wind speed, with loss to risk ratios plotted at the points, failed to show any grouping. In the latter, the same combination of wind speed and direction occurred for a great range of loss to risk ratios.

Correlation between monthly mean shear and loss to risk ratio was also poor. In fact, the year with the highest loss to risk ratio in the twenty-one year period (1953) had a lower wind shear than the year with the lowest loss to risk ratio (1955).

These poor correlations are hardly surprising. On the average, eighty per cent of the hail damage in a given year is caused by the twelve most severe hail days (Summers and Wojtiw, 1971). This means that we are in effect trying to detect conditions which occur on only six days out of thirty-one by looking at monthly mean conditions. It appears that the significant features of the upper air structure on hail days are masked by the averaging process.

In meteorology, many phenomena are explained by talking in terms of mean conditions, such as the mean position of the jet stream. Indications of the present work are that this practice cannot be used with as high a degree of confidence to explain the severity of

hail damage in Alberta as for other phenomena.

4.7 Comment on the Initiation of the Anomalous Sea-surface Temperature Regime

Examination of the cross-sections for July and August of 1957 through 1961 (Figs. B-8 through B-12) reveals that quite a strong monthly mean jet stream occurred as early as 1957, and that as far as the strength of the mean jet is concerned, the anomalous regime appears to have been well established by 1959. The southward displacement is not completely established until 1962. This leads to the question which was responsible for the anomalous sea-surface temperature regime: the formation of the cold pool in the east-central Pacific, which eventually led to the formation of the very strong high in the fall of 1961, or the upper air circulation responding to influences elsewhere and resulting in the production of the cold pool. It certainly does not seem logical that the cold pool would lead to the same atmospheric response as that for the warm pool. Namias (1969) admits that questions such as these are usually unanswerable and that his evidence for the claim that the regime was initiated in the fall of 1961 is circumstantial.

In view of the fact that time constants for oceanic changes are very large compared with the time constants for atmospheric changes, it seems reasonable to conclude that the anomalous sea-surface temperature regime of the sixties may have occurred in response to atmospheric changes beginning as early as 1957.

The July and August monthly mean jet structures for 1967 were considerably weaker than for the previous five years. Again the atmospheric circulation changed before the sea-surface temperature regime did. If a more satisfactory mechanism for the initiation of the anomalous regime is proposed in the future, it seems likely that the role of the atmospheric circulation should be emphasized.

CHAPTER 5

CONCLUSIONS AND RECOMMENDATIONS

5.1 Conclusions

Concurrent with the North Pacific sea-surface temperature anomaly from the fall of 1961 to the winter of 1967-68 was a marked reduction in hail damage in Alberta for the summers of 1962 through 1967. Neglecting any effects which have not been considered, this suggests that either the sea-surface temperature anomaly was responsible for the reduction, or that the mechanism responsible for the anomaly also caused the reduction in hail damage.

The effect on the summer upper air circulation over Alberta was a southward shift of at least one grid interval (381 km) and a marked intensification of the jet maximum. Averaged over the period 1962-67, the increase in the mean jet maximum was found to be approximately eleven and seven ms^{-1} for July and August respectively. Some evidence was found to support the hypothesis that the hail damage moved southward with the mean jet stream.

Attempts at correlation of hail damage with parameters such as monthly mean upper air wind speed, direction, and shear produced no useful diagnostic tools. This may be a result of the discrepancy in the time scales. The storms responsible for the hail

damage have lifetimes measured in terms of hours whereas the averaging time used for the upper air data is one month.

Correlation between hail damage and monthly mean precipitation gave no proof to support the commonly held belief that high spring precipitation leads to high summer hail damage. Good correlation was found to exist between annual loss to risk ratios and August precipitation because the latter is primarily convective in nature. These findings imply that low level moisture advection is the primary source of moisture for the development of severe convective storms.

5.2 Recommendations

The monthly mean upper air structure and sea-surface temperature in the North Pacific should be closely monitored on a routine basis. The former is by far the easier of the two. In the event of a recurrence of the anomalous regime, a reduction in hail damage in Alberta can be forecast on a yearly basis until the regime breaks down again.

Teleconnection has explained anomalies in equatorial rainfall, colder winters in the eastern two-thirds of the United States, drought in the North-eastern United States, and a reduction in hail damage in Alberta. Undoubtedly there are many more phenomena that can be related to anomalous air-sea interactions, and further research is warranted. Aside from producing new long range forecast tools, better understanding of the general circulation and insight into how such climatic variations could be incorporated into present or future numerical weather prediction models would also be gained.

BIBLIOGRAPHY

Bergthórssen, P., and B. R. Döös, 1955: Numerical weather maps analysis. Tellus, 7, 329-340.

Bjerknes, J., 1969: Atmospheric teleconnections from the equatorial Pacific. Monthly Weather Review, 97, 163-172.

Cressman, G. P., 1959: An operational objective analysis system. Monthly Weather Review, 87, 367-374.

Glahn, H. R., and G. W. Hollenbach, 1959: An Operationally Oriented Small-scale 500 mb Height Analysis Program. U.S. Dept. of Commerce, Essa Technical Memorandum WBTM TDL 19.

Helland-Hansen, B., and F. Nansen, 1920: Temperature variations in the North Atlantic Ocean and in the atmosphere, introductory studies on the causes of climatological variations. Miscellaneous Collections, Vol. 70, No. 4, Publication 2537, Smithsonian Institute, Washington, D.C., 408 pp.

Holloway, J. L., Jr., 1958: Smoothing and filtering of time series and space fields. Advances in Geophysics, 4, 351-389.

Jacobs, W. C., 1951: The energy exchange between sea and atmosphere and some of its consequences. Bulletin of the Scripps Institute of Oceanography, La Jolla, Calif., 6, 122 pp.

Keeping, E. S., 1962: Introduction to Statistical Inference. Princeton, D. Van Nostrand, 451 pp.

Linton, J. C., J. E. Campbell, J. Dublin, R. F. Hopkinson, R. C. Jacobs, and D. L. Oracheski, 1971: An Objective Analysis Program. Unpublished manuscript.

Namias, J., 1966: Nature and possible causes of the North-eastern United States drought during 1962-65. Monthly Weather Review, 94, 543-554.

Namias, J., 1969: Seasonal interactions between the North Pacific Ocean and the atmosphere during the 1960's. Monthly Weather Review, 97, 173-192.

Summers, P. W., 1966: Note on the Use of Hail Insurance Data for the Evaluation of Hail Suppression Techniques. Research Council of Alberta, Information Series No. 52, 25 pp.

Summers, P. W., and A. H. Paul, 1967: Some climatological characteristics of hailfall in central Alberta. Stormy Weather Group Scientific Report MW-57. Montreal; McGill University, 17-26.

Summers, P. W., and L. Wojtiw, 1971: The economic impact of hail damage in Alberta, Canada, and its dependence on various hailfall parameters. Proc. Seventh Conf. on Severe Local Storms, Amer. Meteor. Soc. Boston, 158-163.

Thomasell, A., Jr., and J. G. Welsh, 1962: Objective analysis of sea level pressure, surface temperature, dew point, and wind. Tech. Publication 19, Contract FAA/BRD-363. The Travellers Research Centre, Inc., 87 pp.

von Arx, W. S., 1962: An Introduction to Physical Oceanography. Reading, Addison-Wesley Publishing Co., 422 pp.

APPENDIX A

EXAMPLES OF OBJECTIVE ANALYSIS OUTPUT

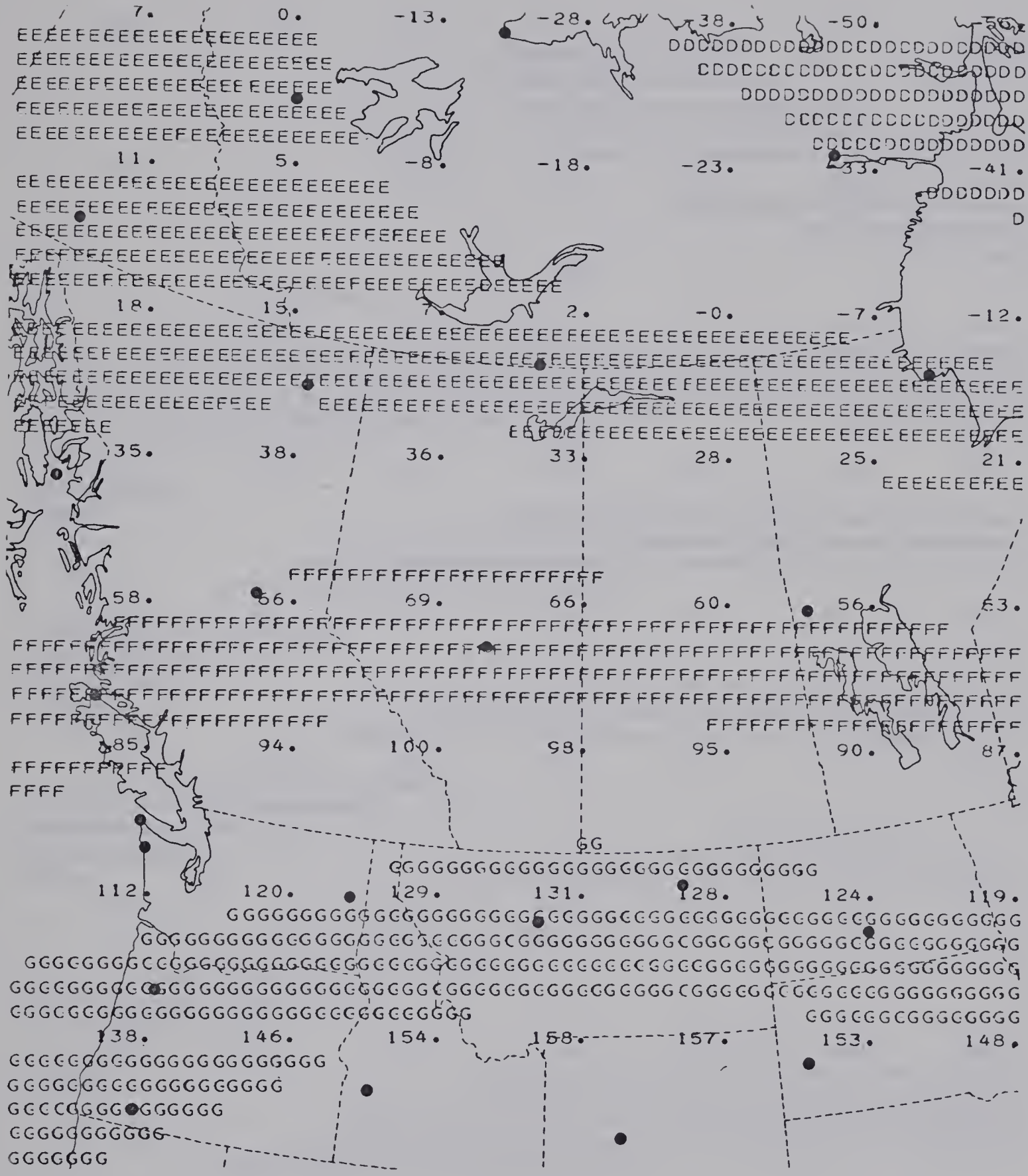

Fig. A-1 Analysis of 700 mb. monthly mean heights for July 1970.

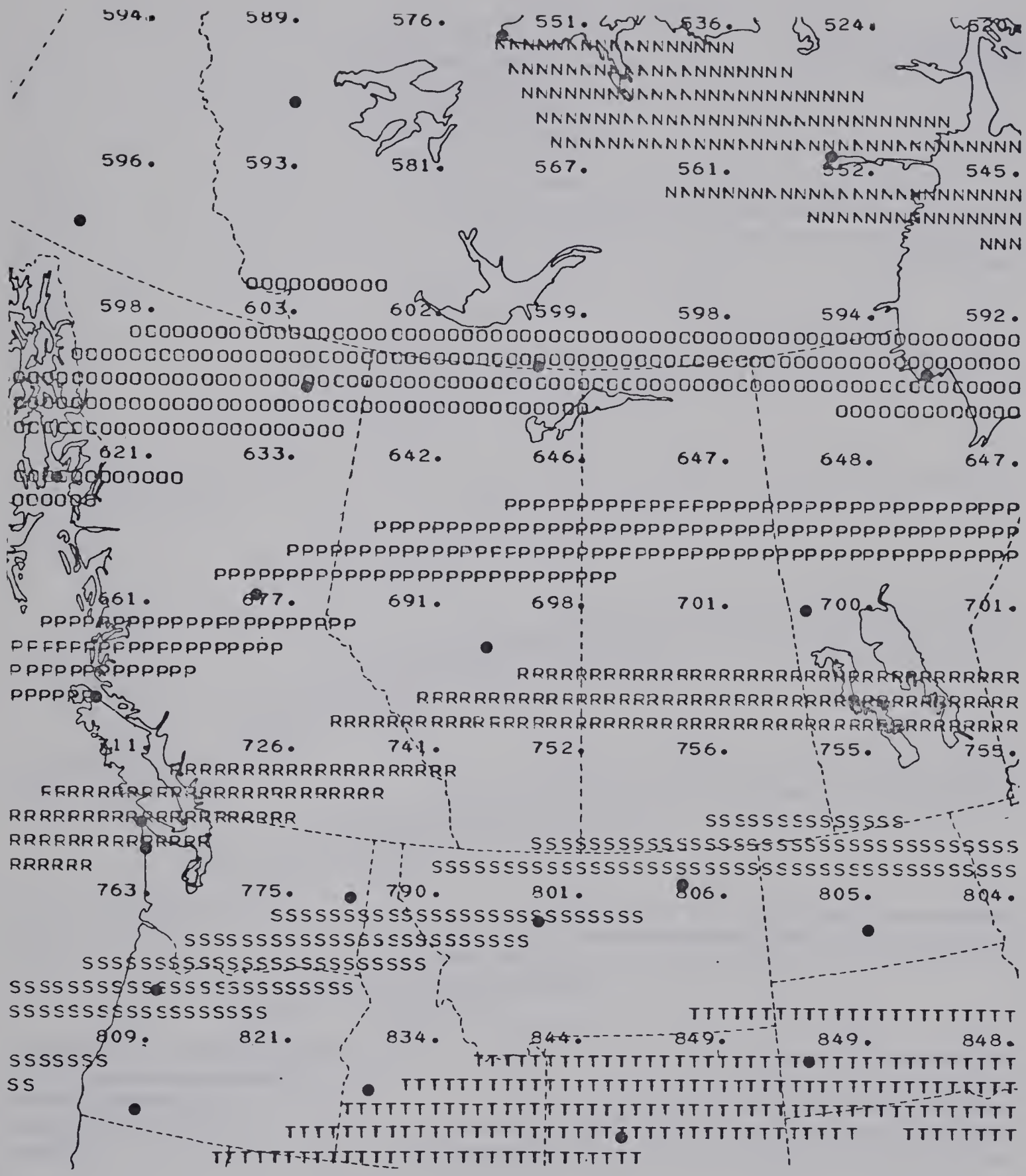

Fig. A-2 Analysis of 500 mb. monthly mean heights for July 1970.

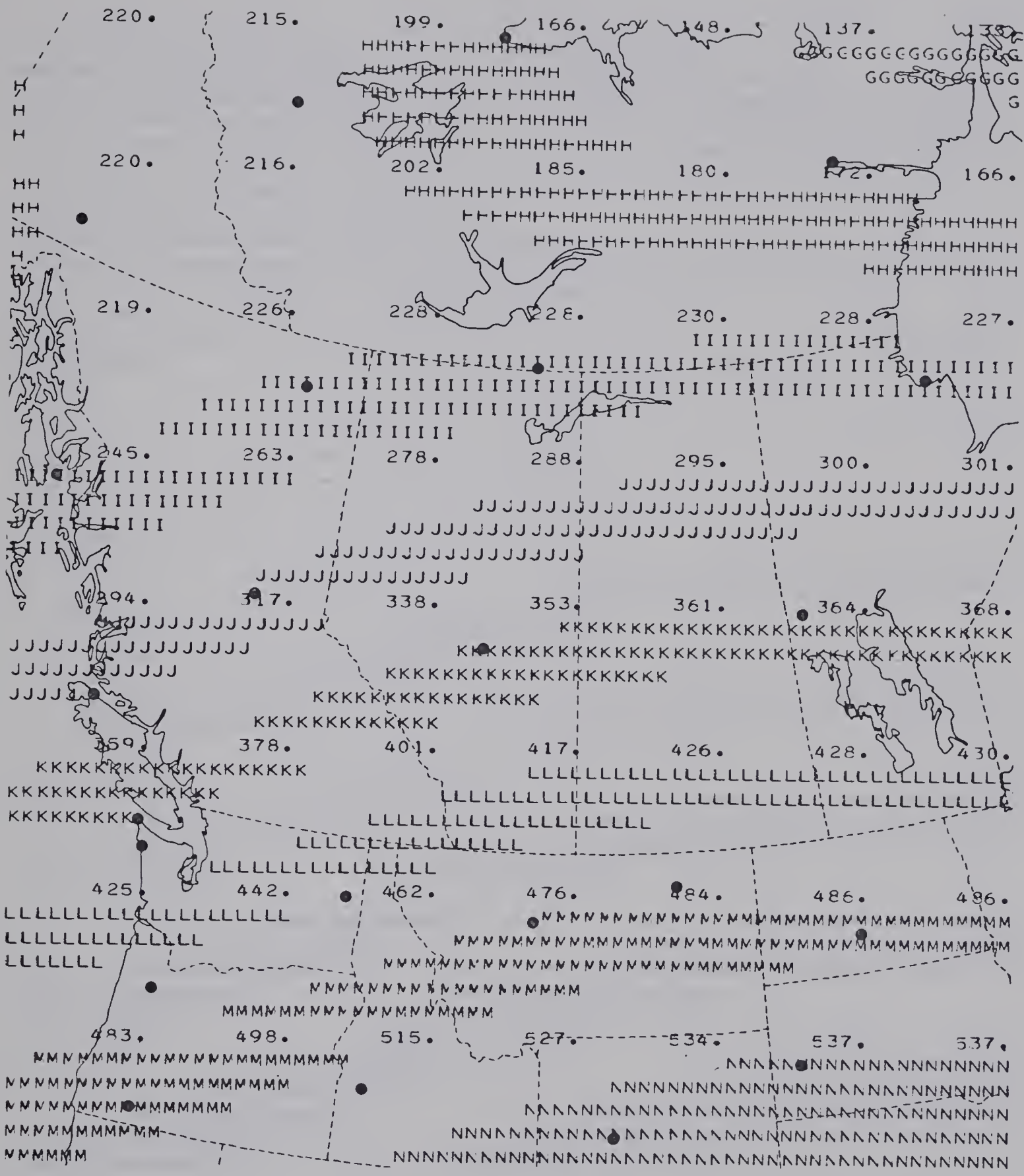

Fig. A-3 Analysis of 400 mb. monthly mean heights for July 1970.

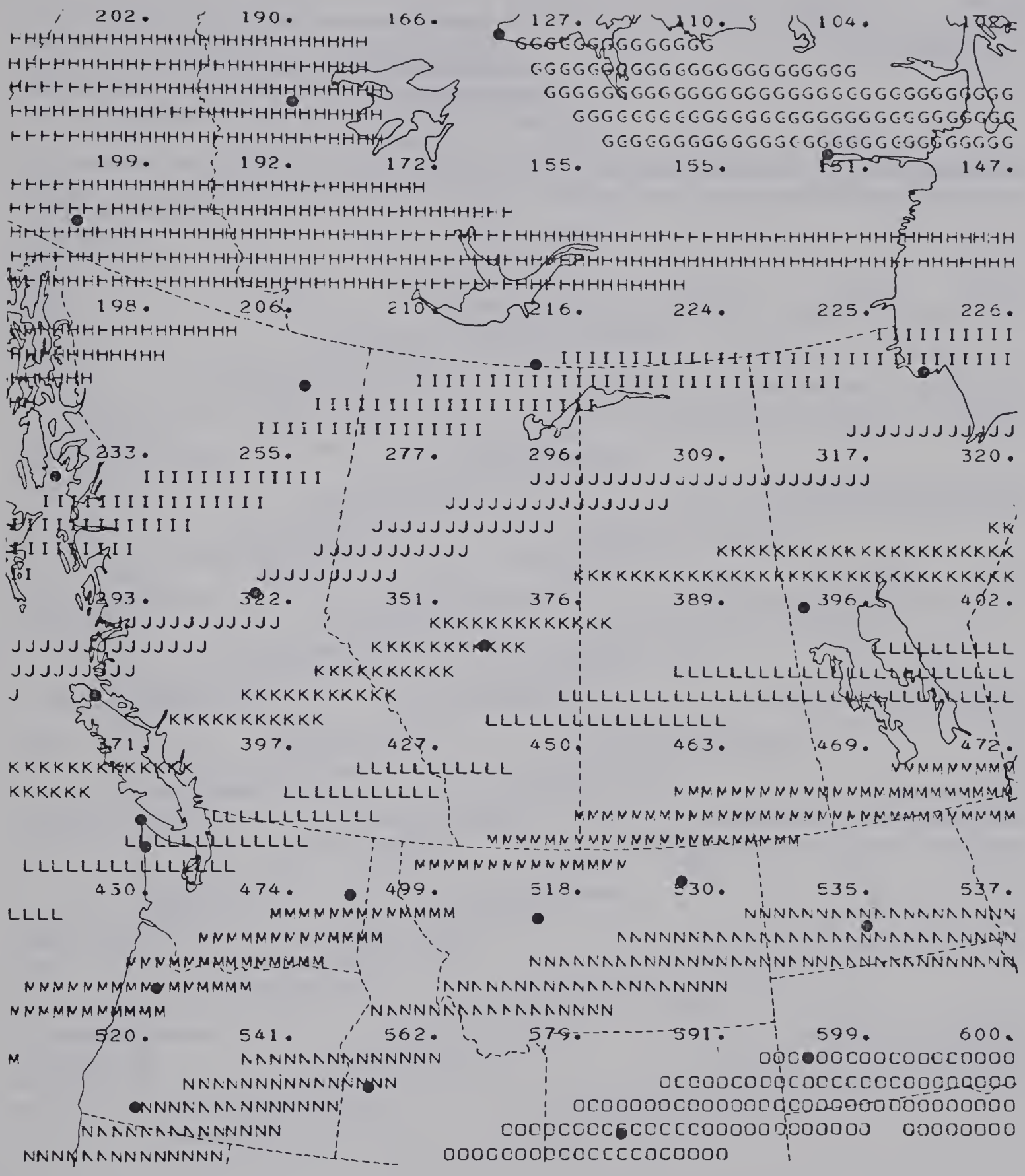

Fig. A-4 Analysis of 300 mb. monthly mean heights for July 1970.

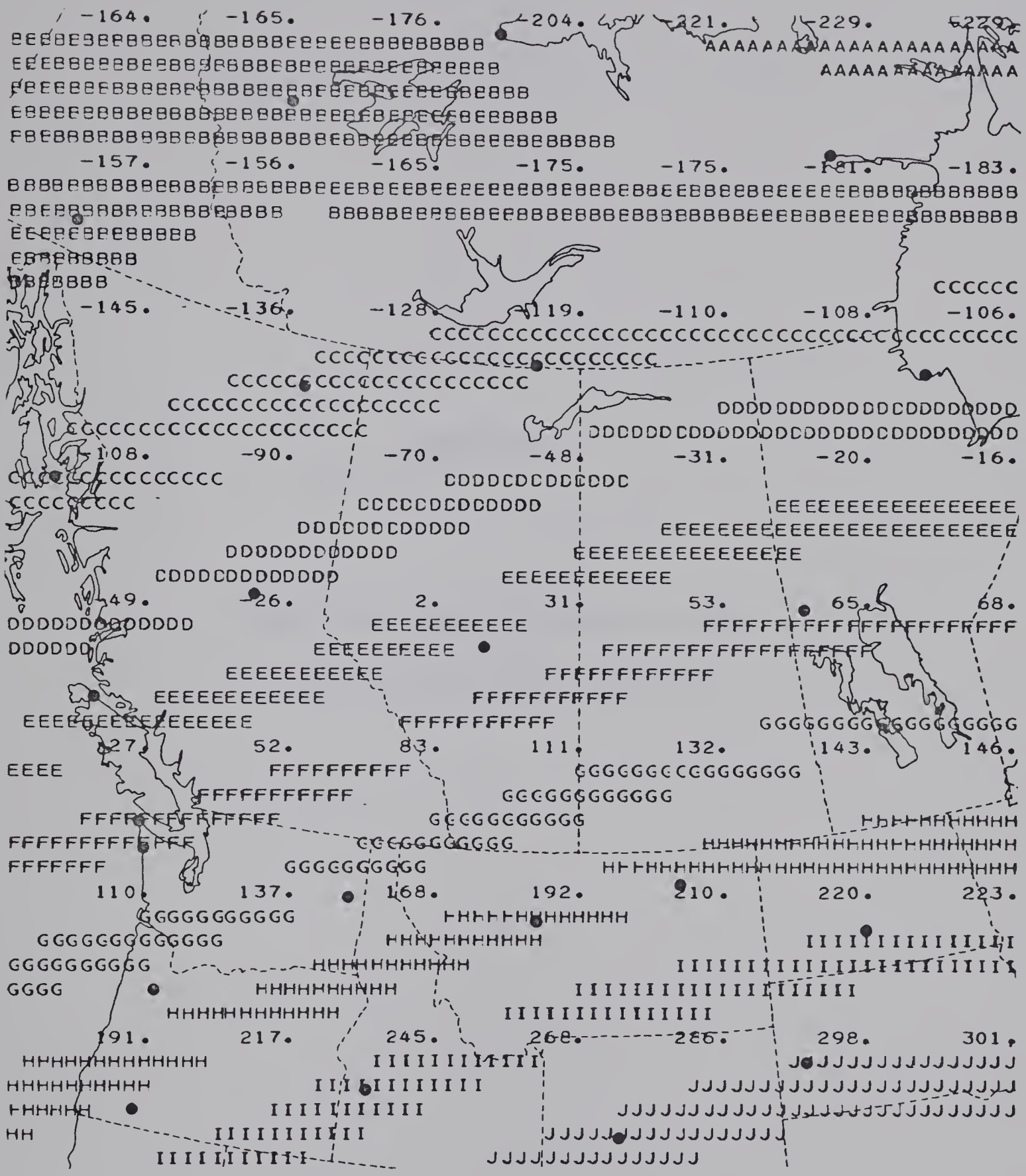

Fig. A-5 Analysis of 200 mb. monthly mean heights for July 1970.

APPENDIX B

MONTHLY MEAN CROSS-SECTIONS FOR JULY AND AUGUST FOR PERIOD 1950-1970

LEGEND FOR INTERPRETATION OF CROSS-SECTIONS

DDD ← wind direction in degrees

FF.F ← wind speed in ms^{-1}

———— isotachs, labelled in ms^{-1}

- - - - - - - isogons, labelled in degrees

Station Identifiers

SM	Fort Smith, N.W.T.
EG	Edmonton, Alta.
QF	Penhold, Alta.
YC	Calgary, Alta.
QL	Lethbridge, Alta.
GTF	Great Falls, Mont.

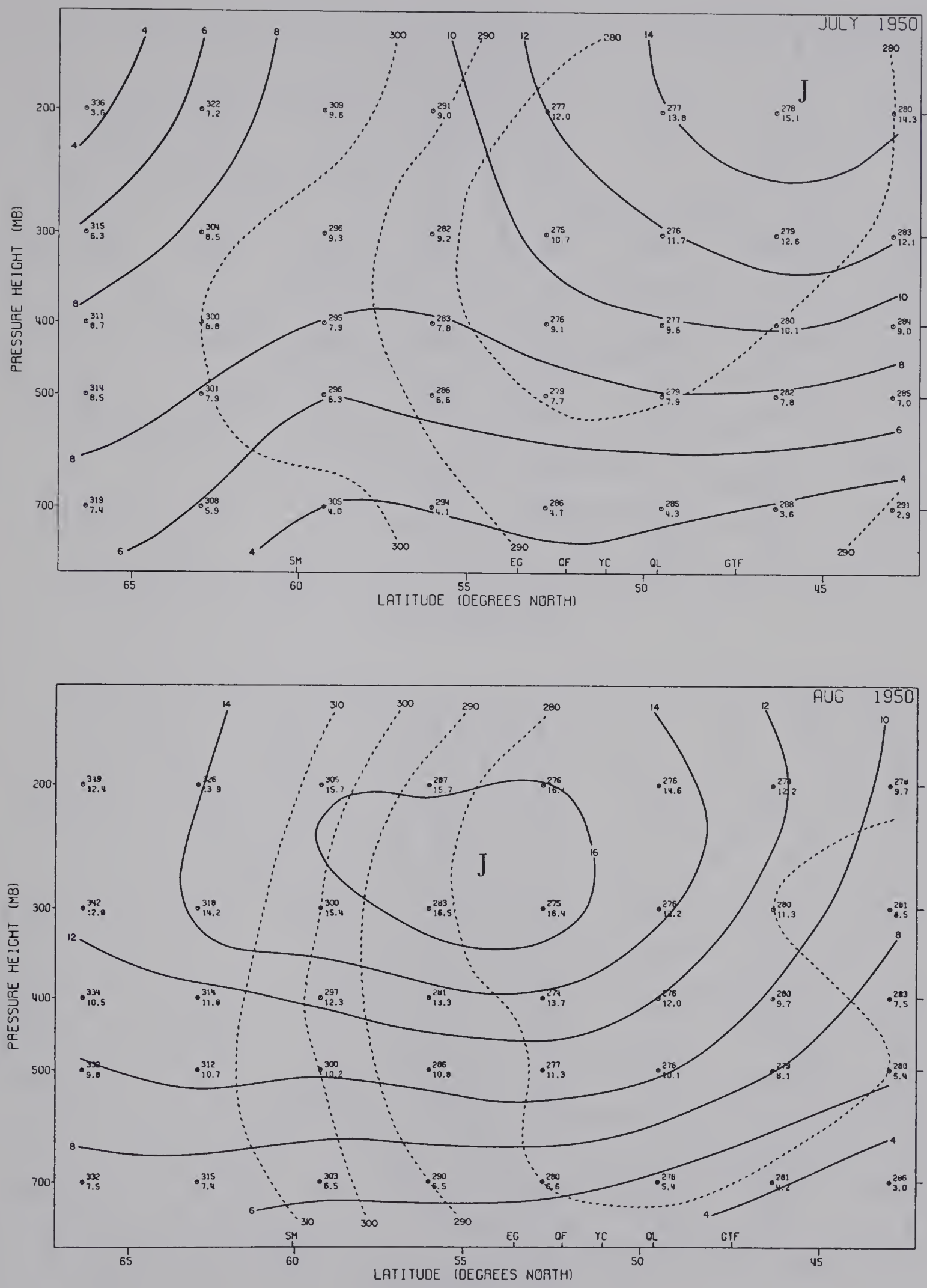

Fig. B-1 Monthly mean cross-sections for July and August, 1950.

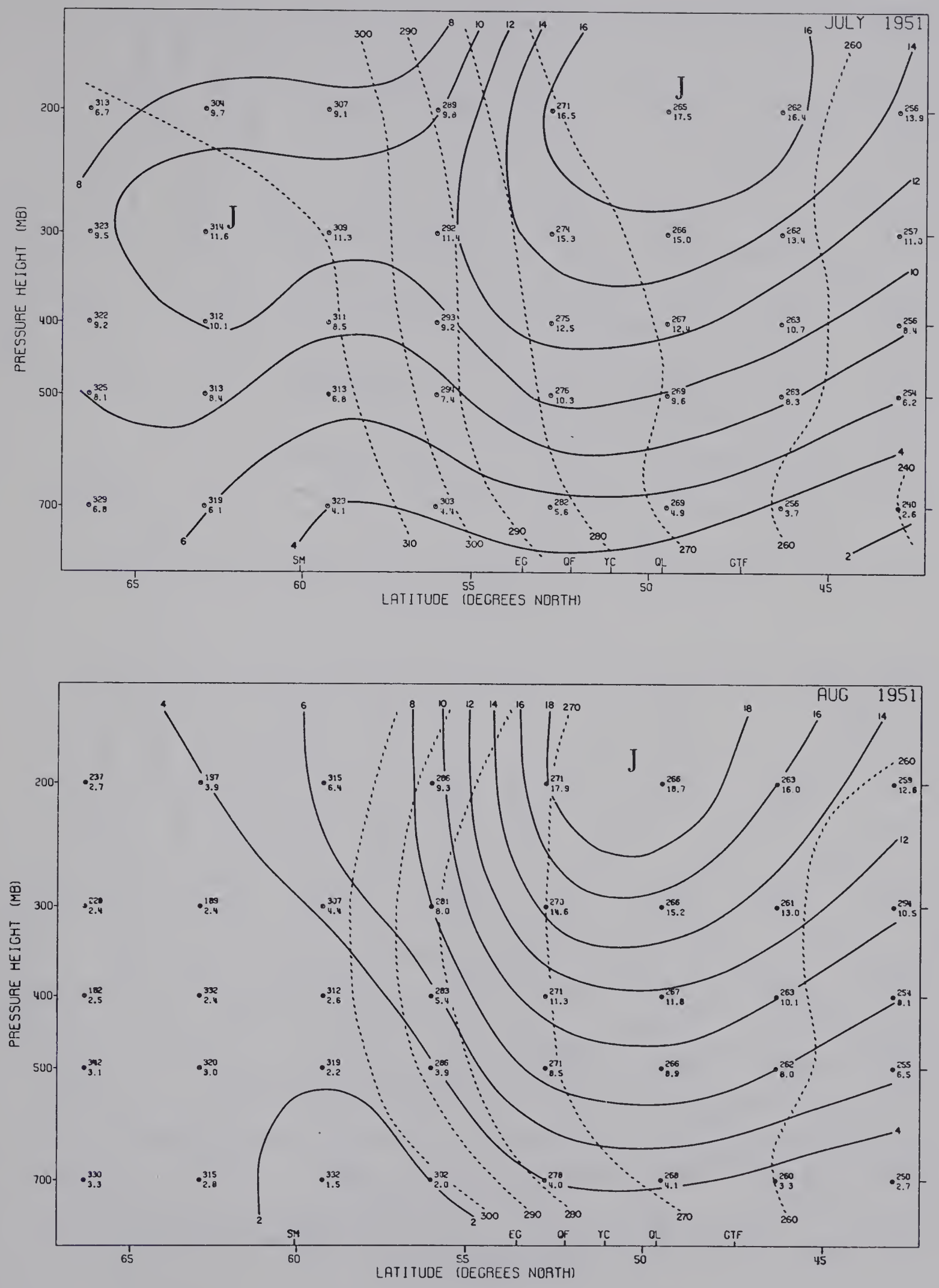

Fig. B-2 Monthly mean cross-sections for July and August, 1951.

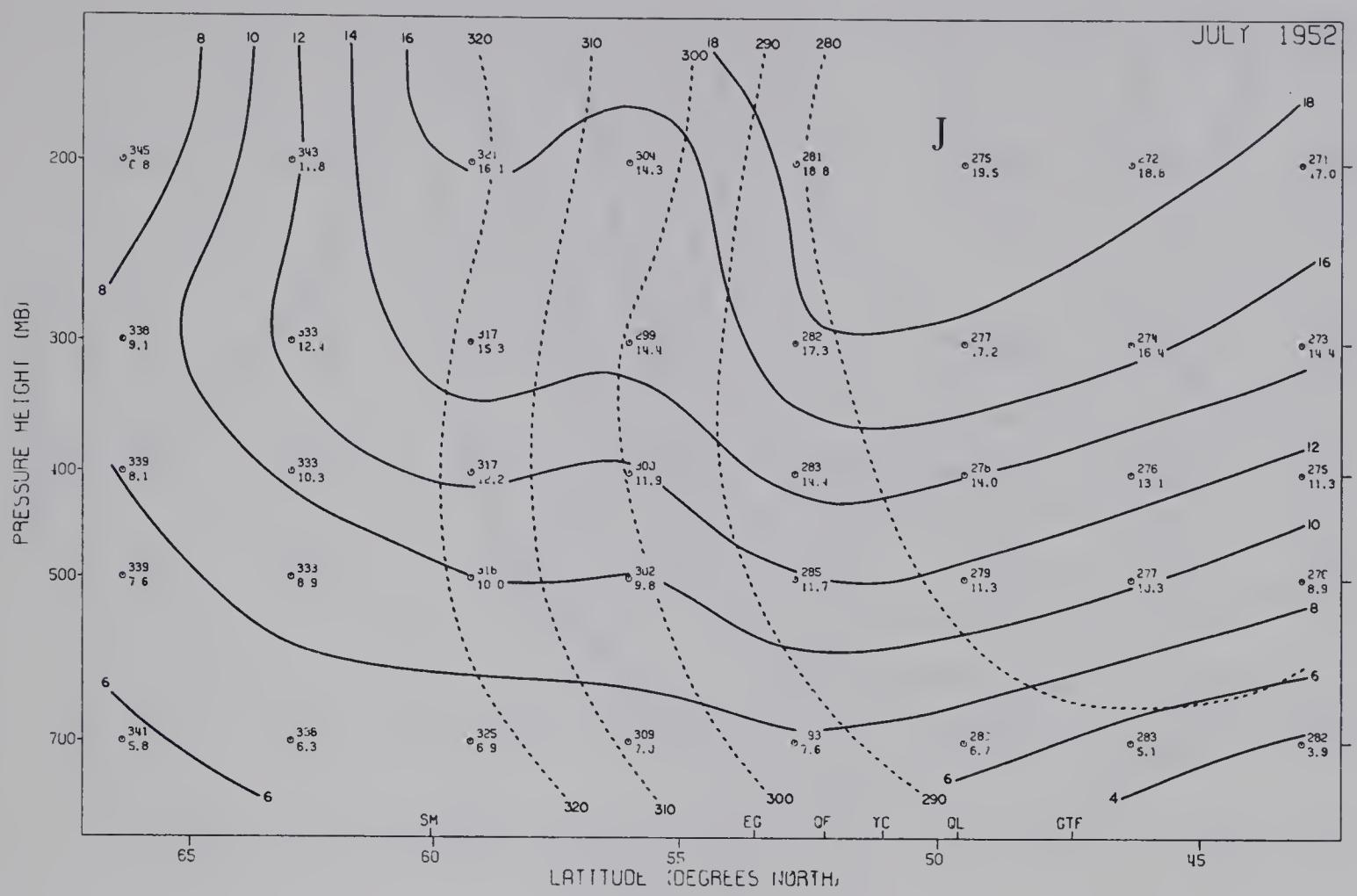

Fig. B-3 Monthly mean cross-sections for July and August, 1952.

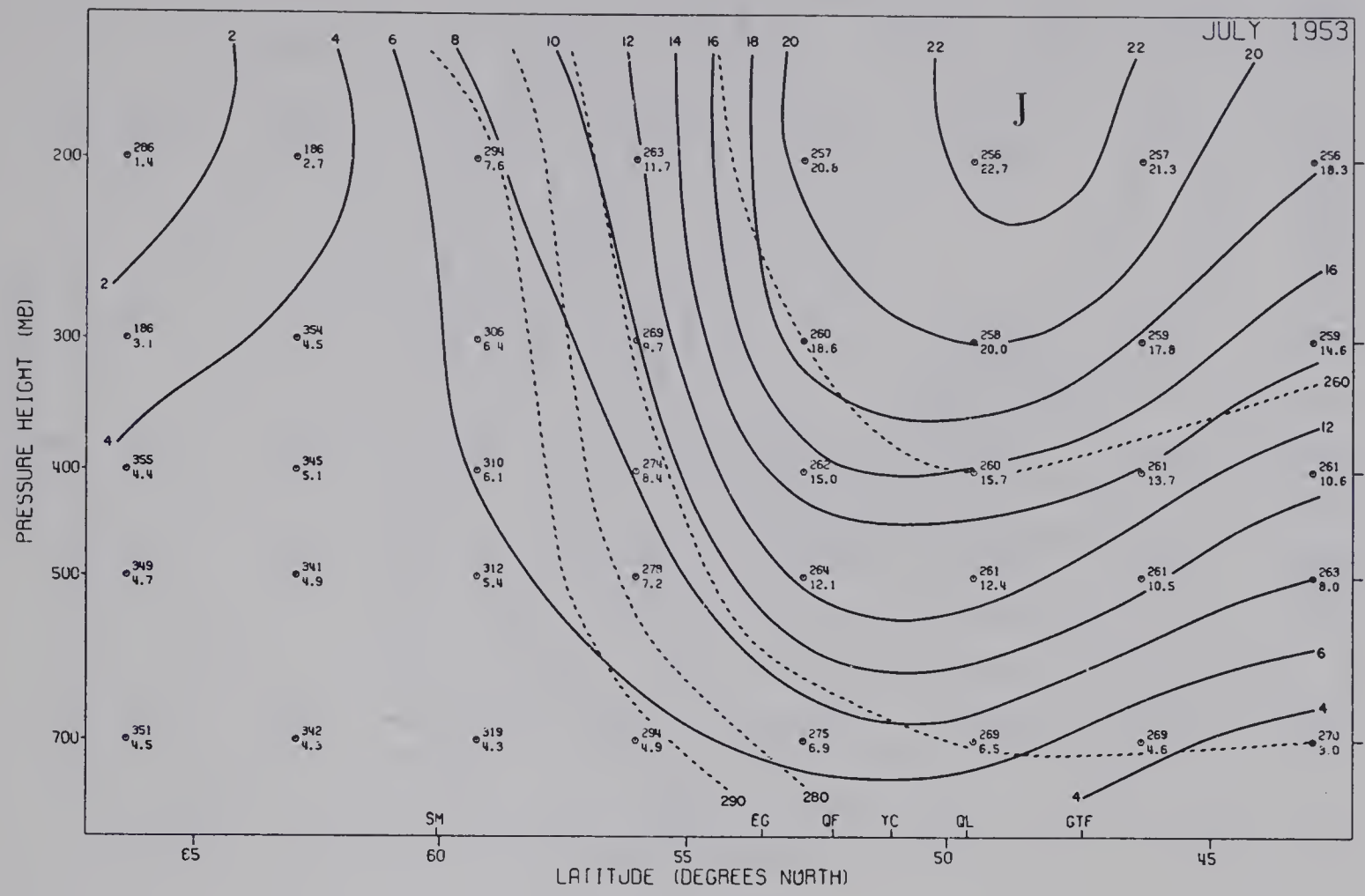

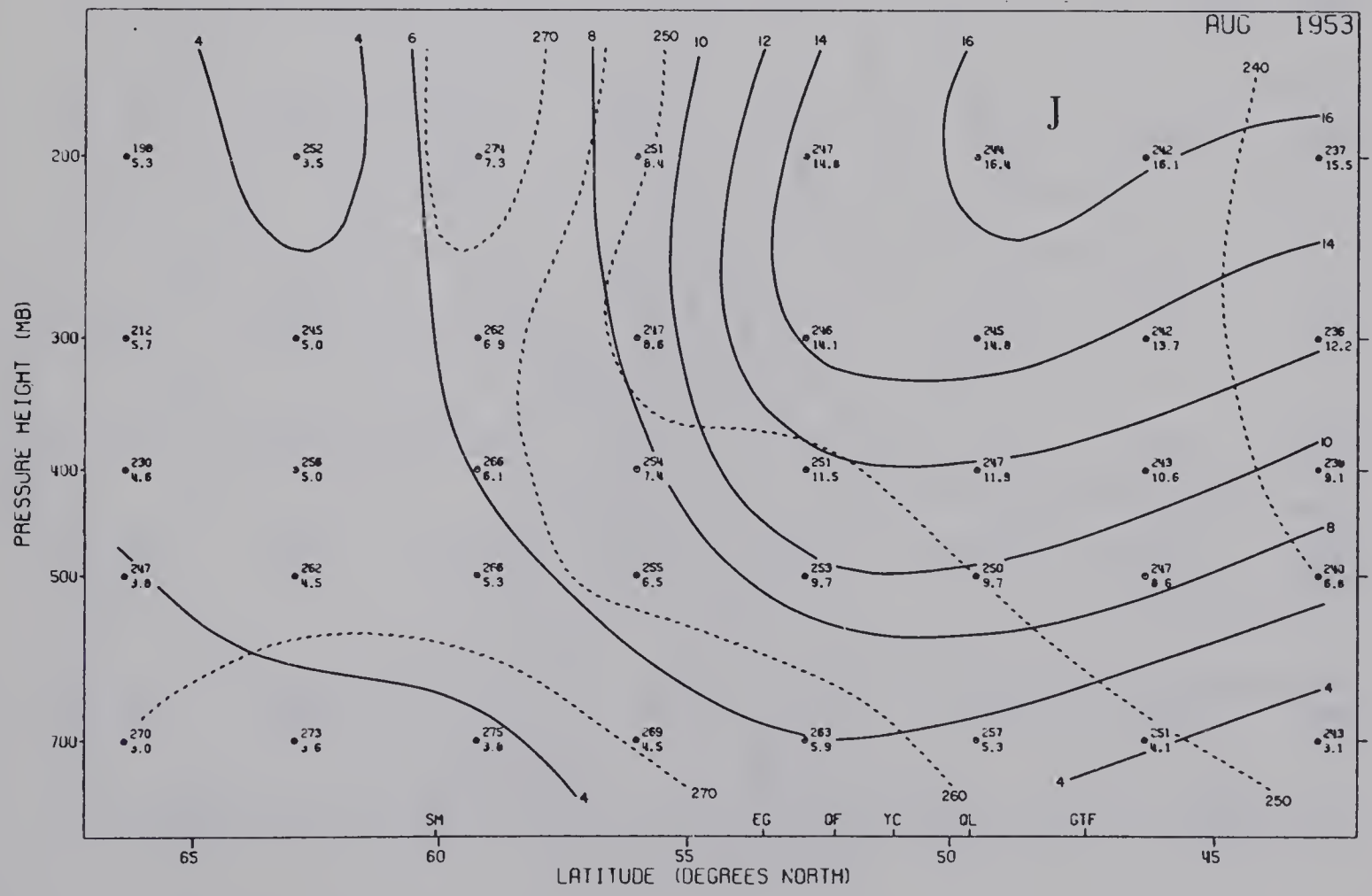

Fig. B-4 Monthly mean cross-sections for July and August, 1953.

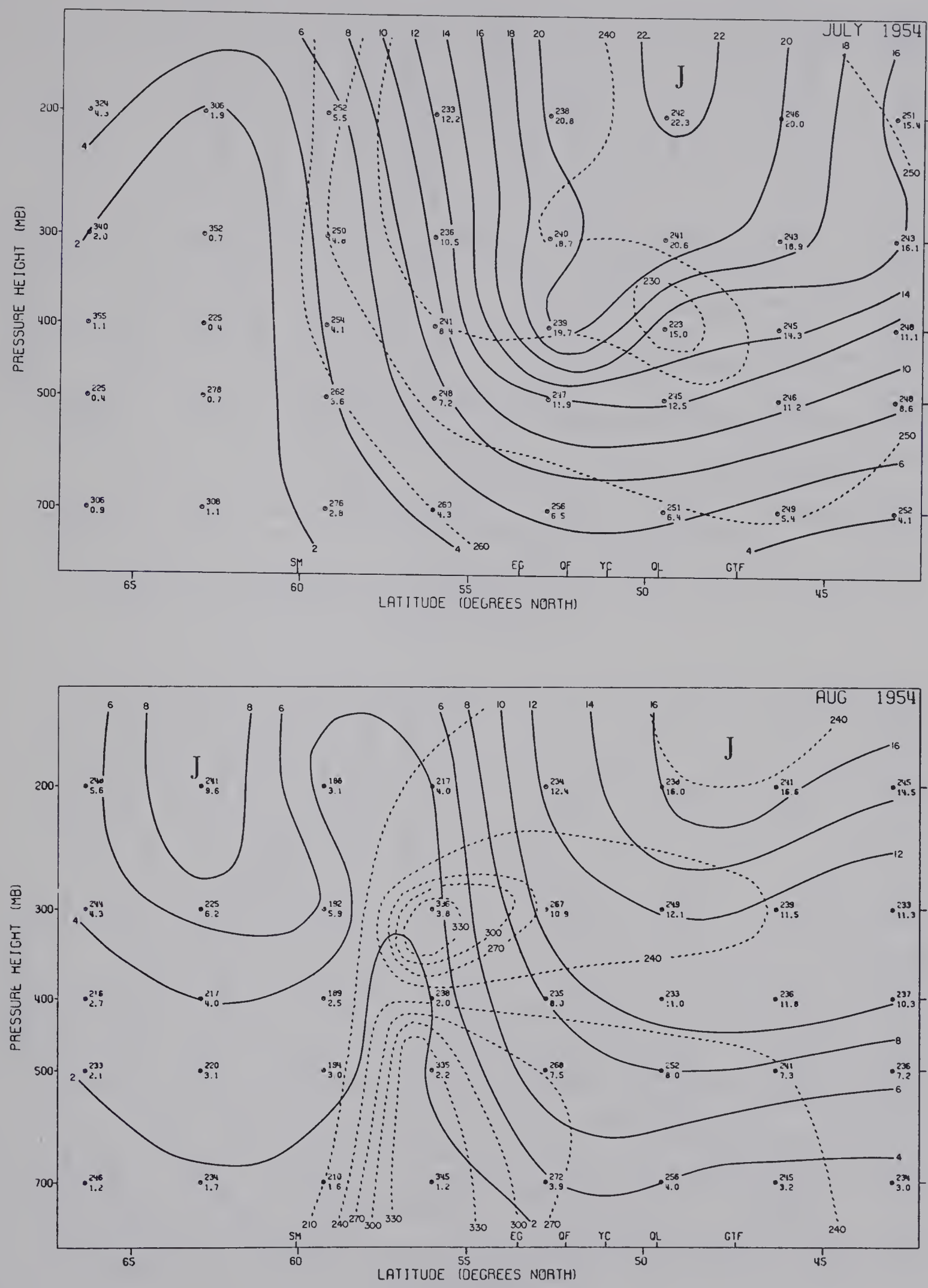

Fig. B-5 Monthly mean cross-sections for July and August, 1954.

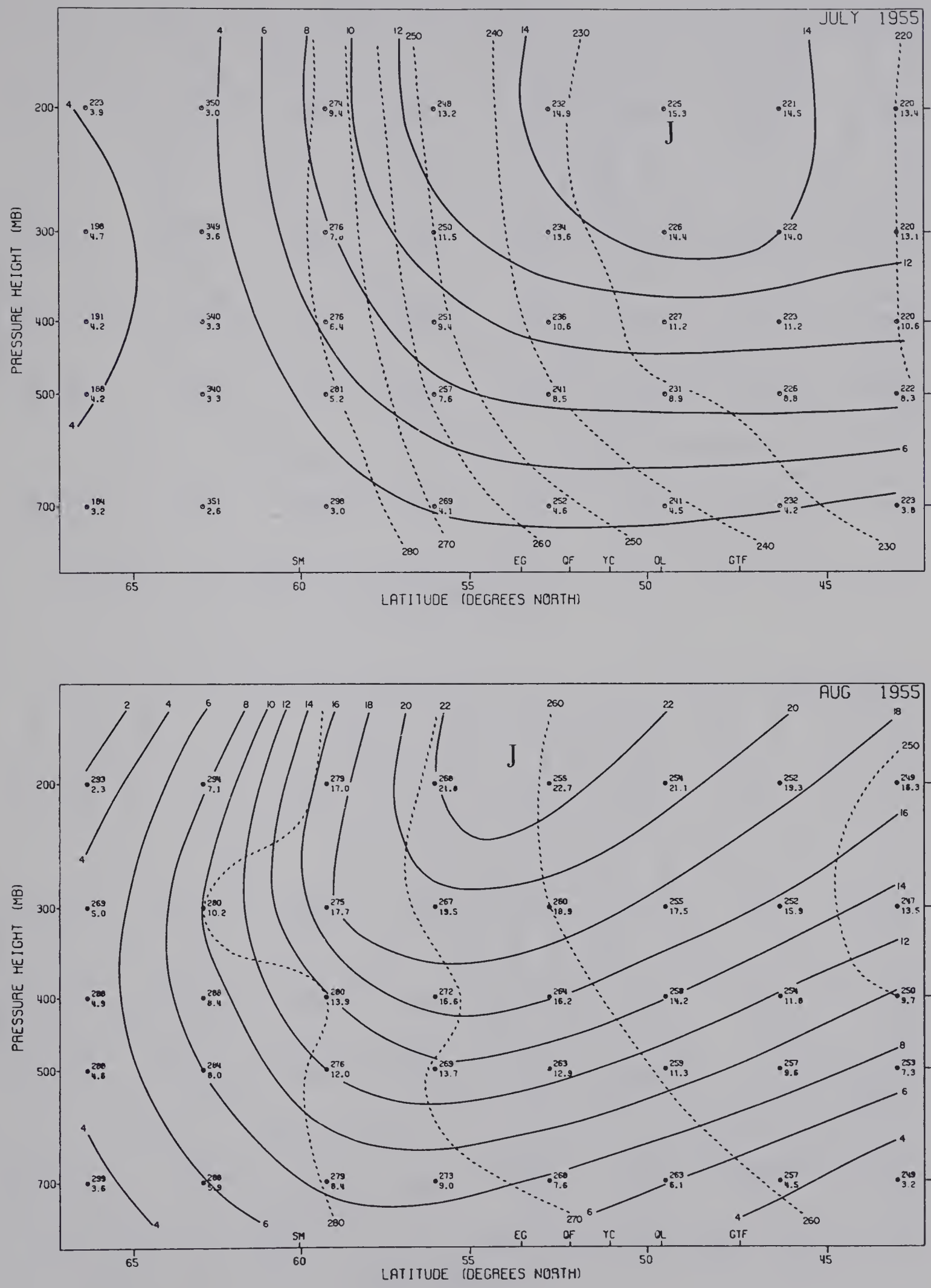

Fig. B-6 Monthly mean cross-sections for July and August, 1955.

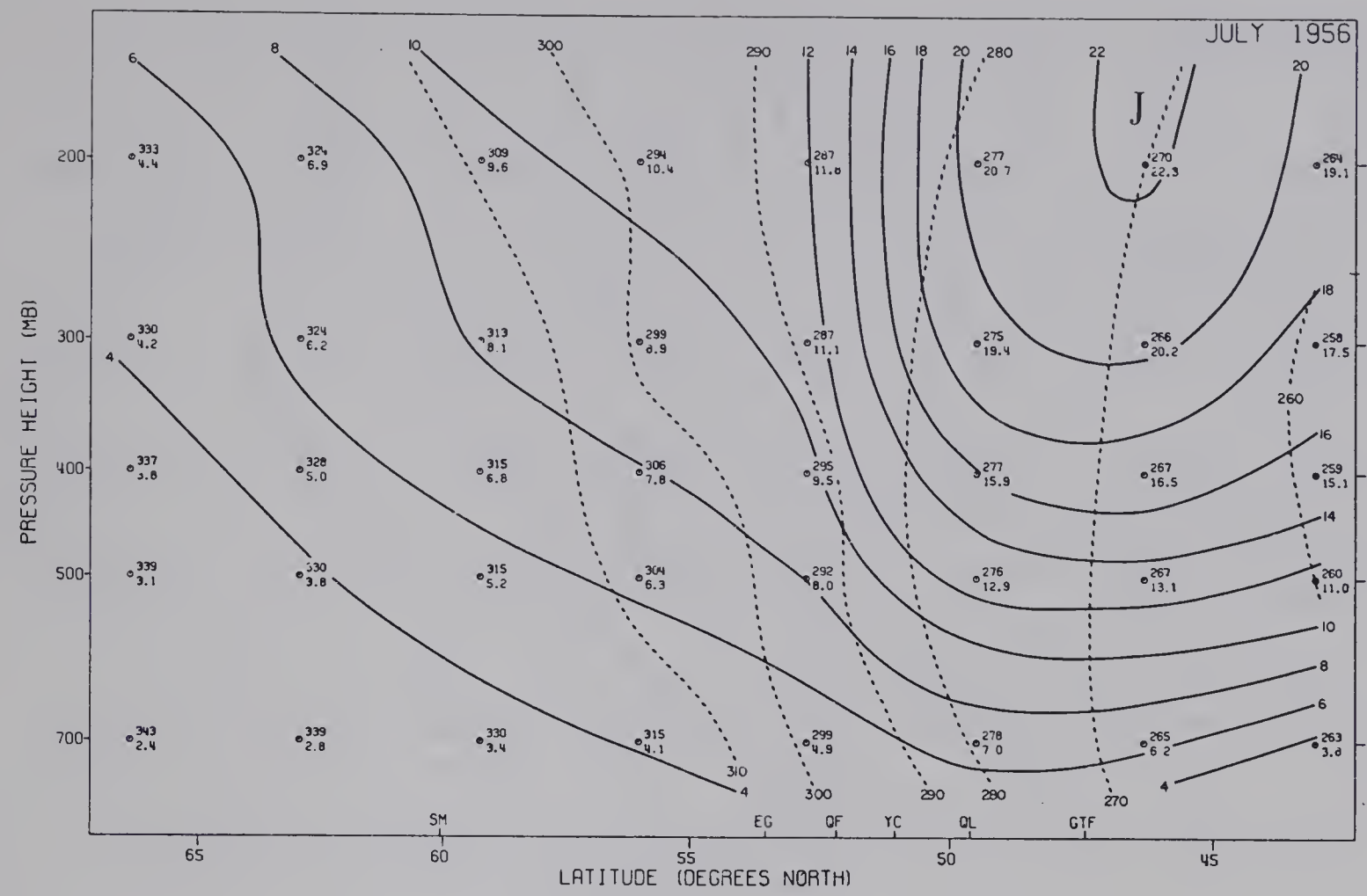

Fig. B-7 Monthly mean cross-sections for July and August, 1956.

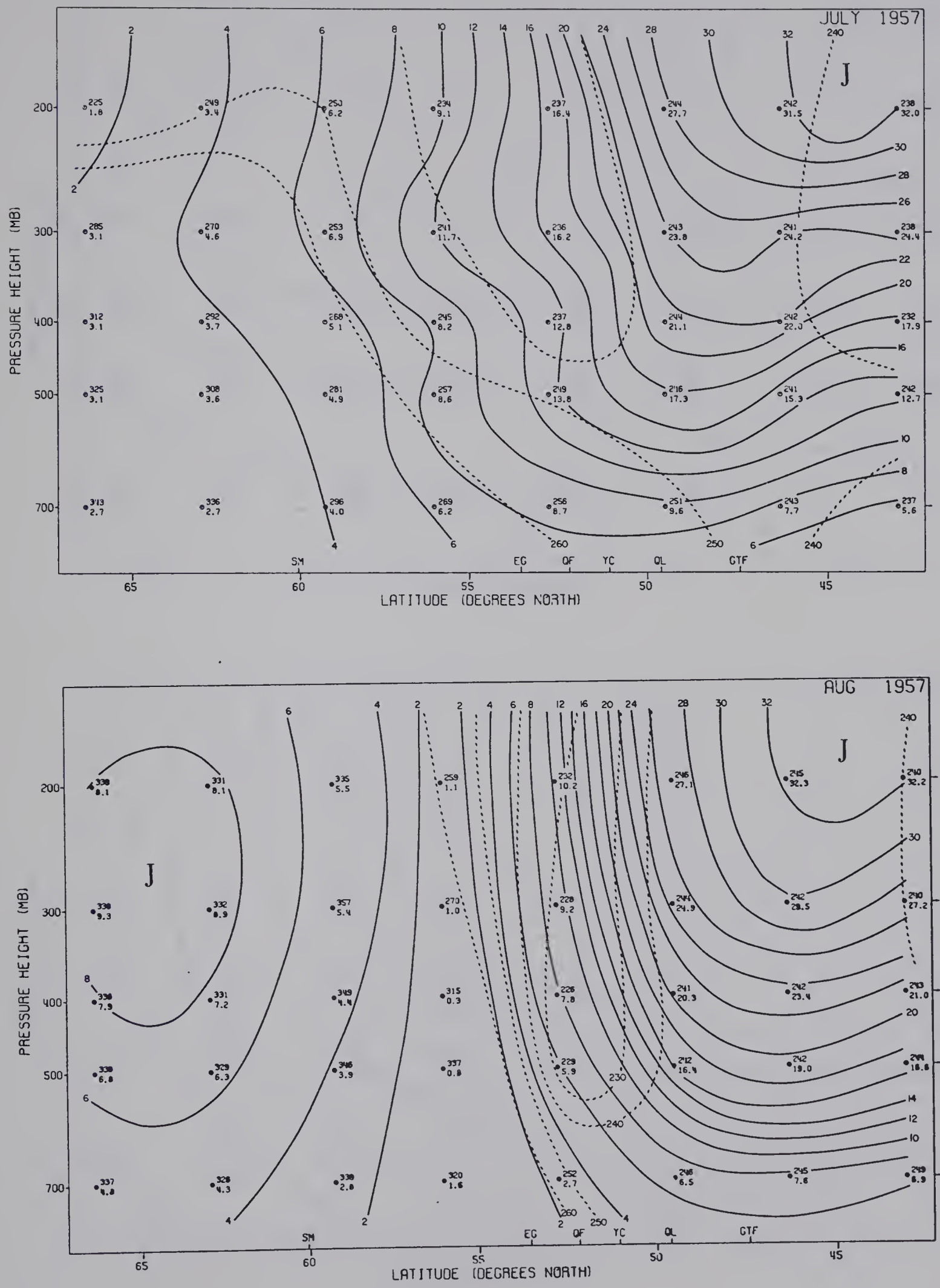

Fig. B-8 Monthly mean cross-sections for July and August, 1957.

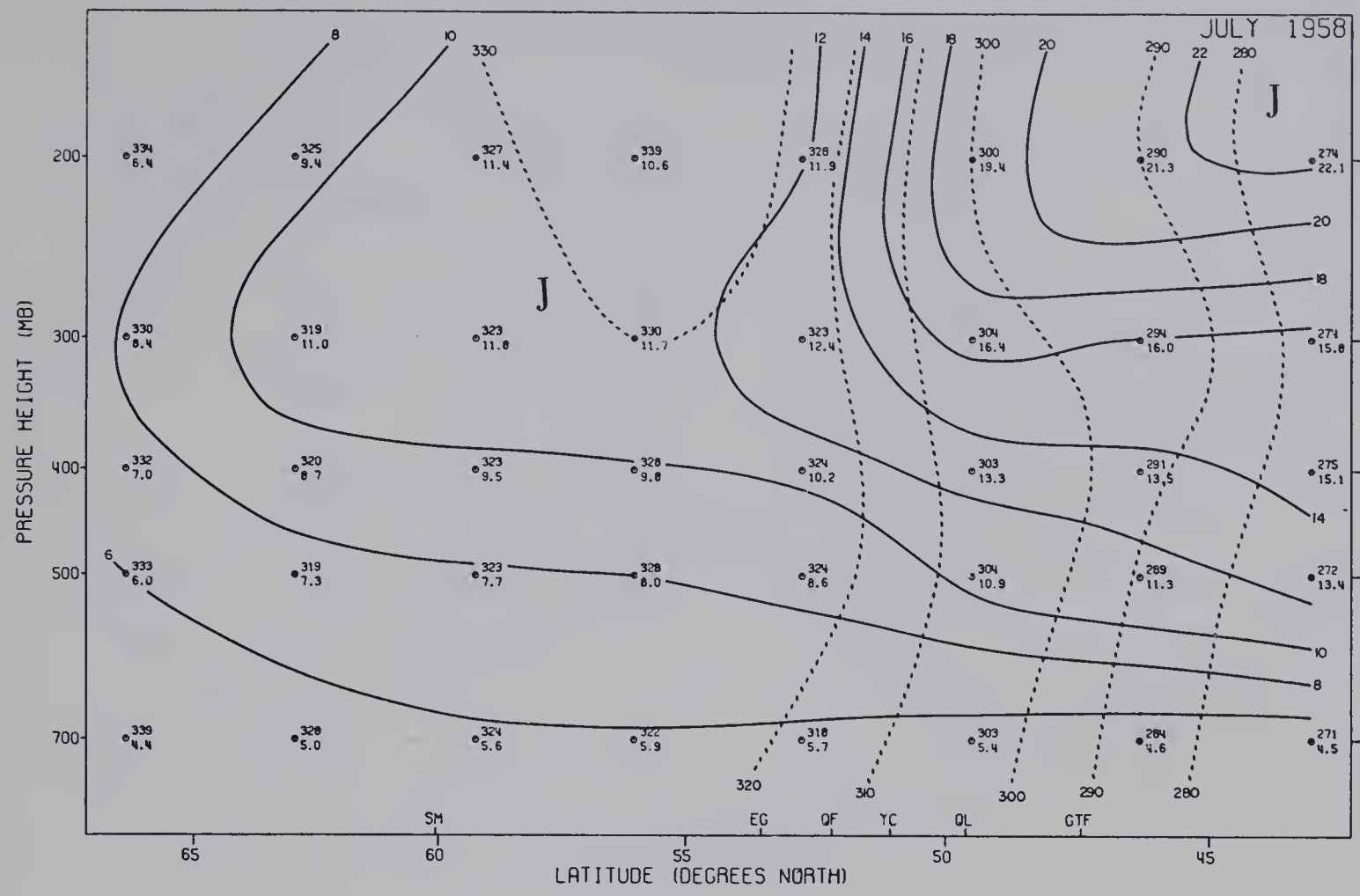

Fig. B-9 Monthly mean cross-sections for July and August, 1958.

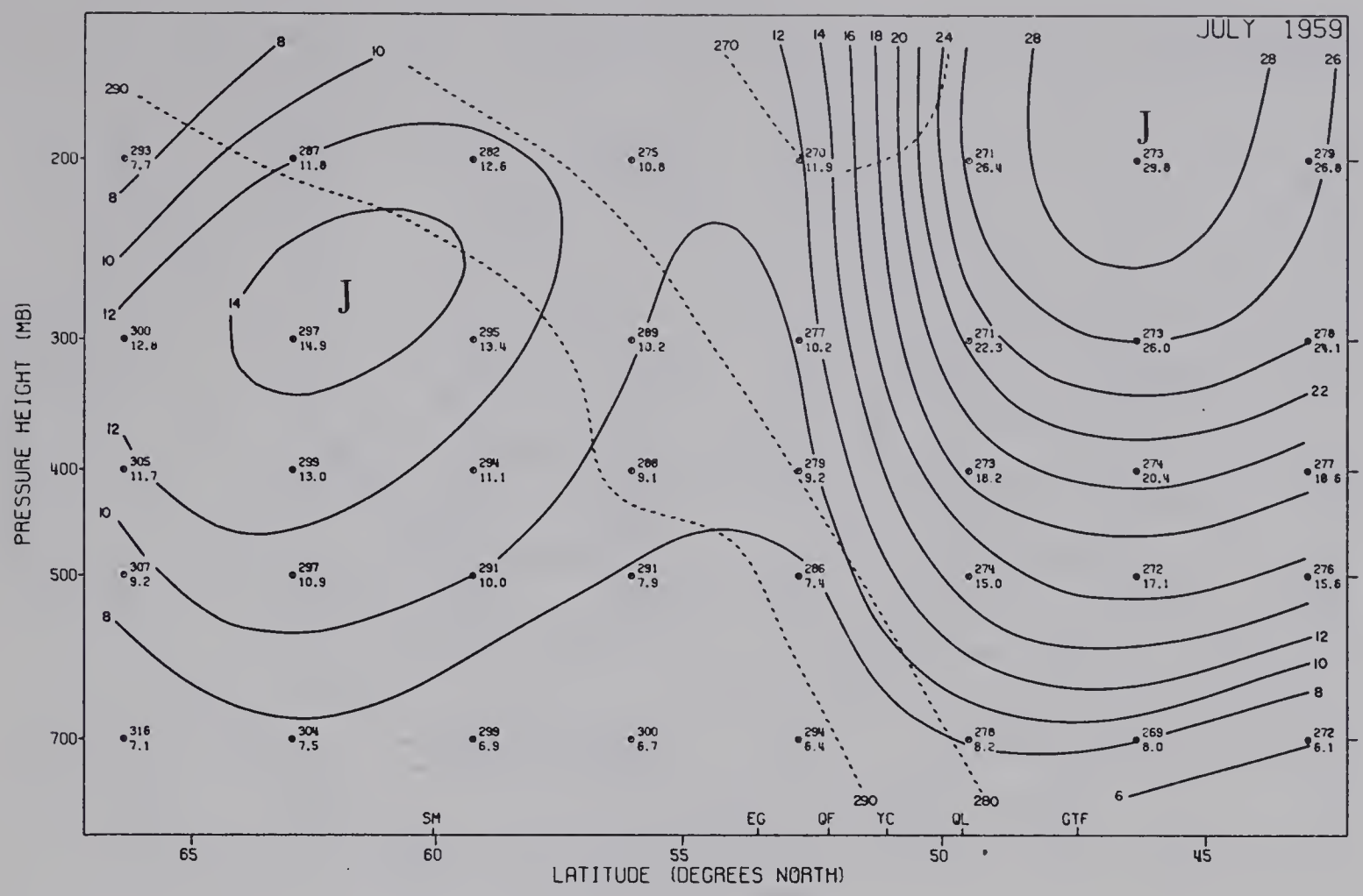

Fig. B-10 Monthly mean cross-sections for July and August, 1959.

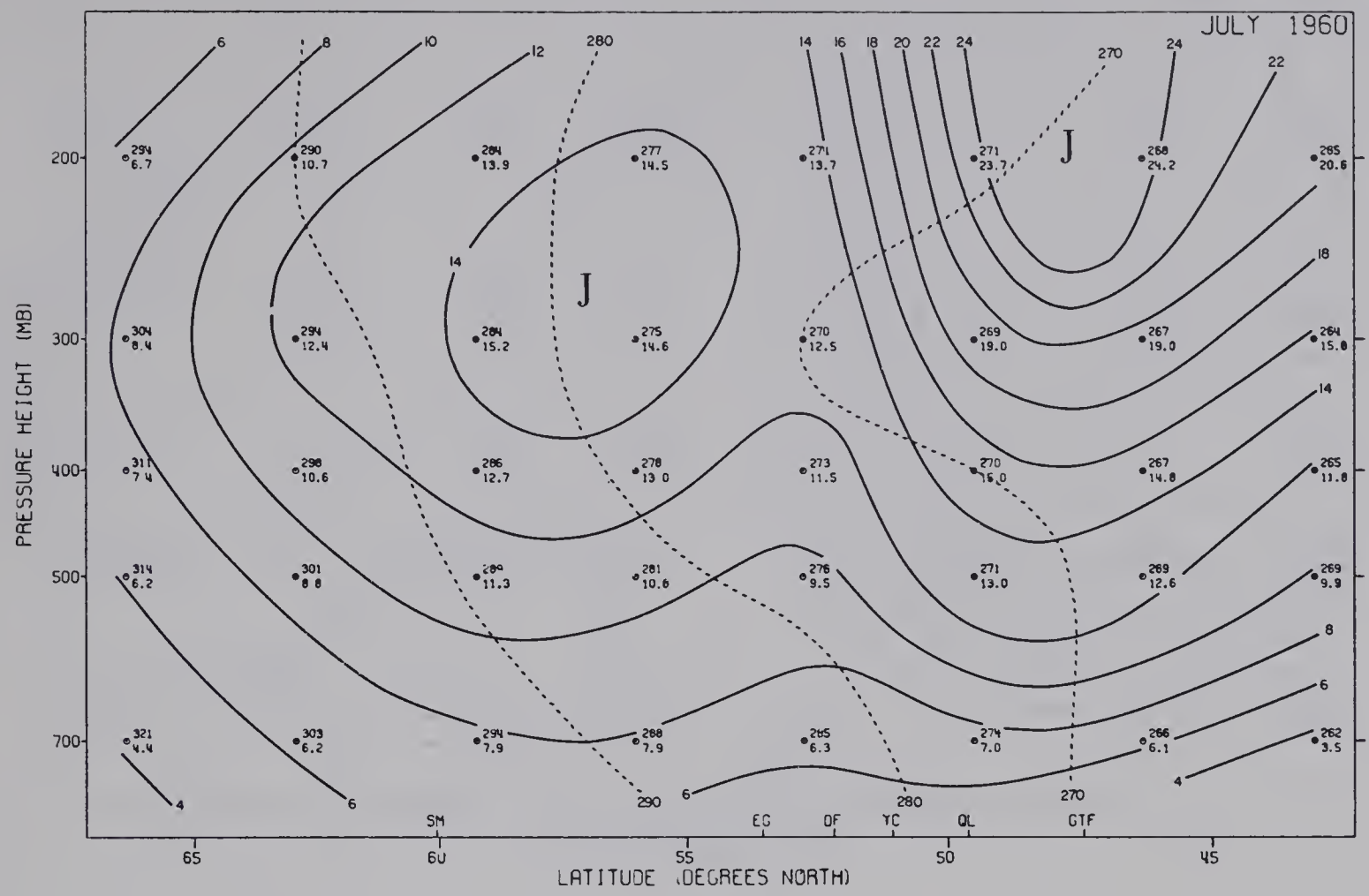

Fig. B-11 Monthly mean cross-sections for July and August, 1960.

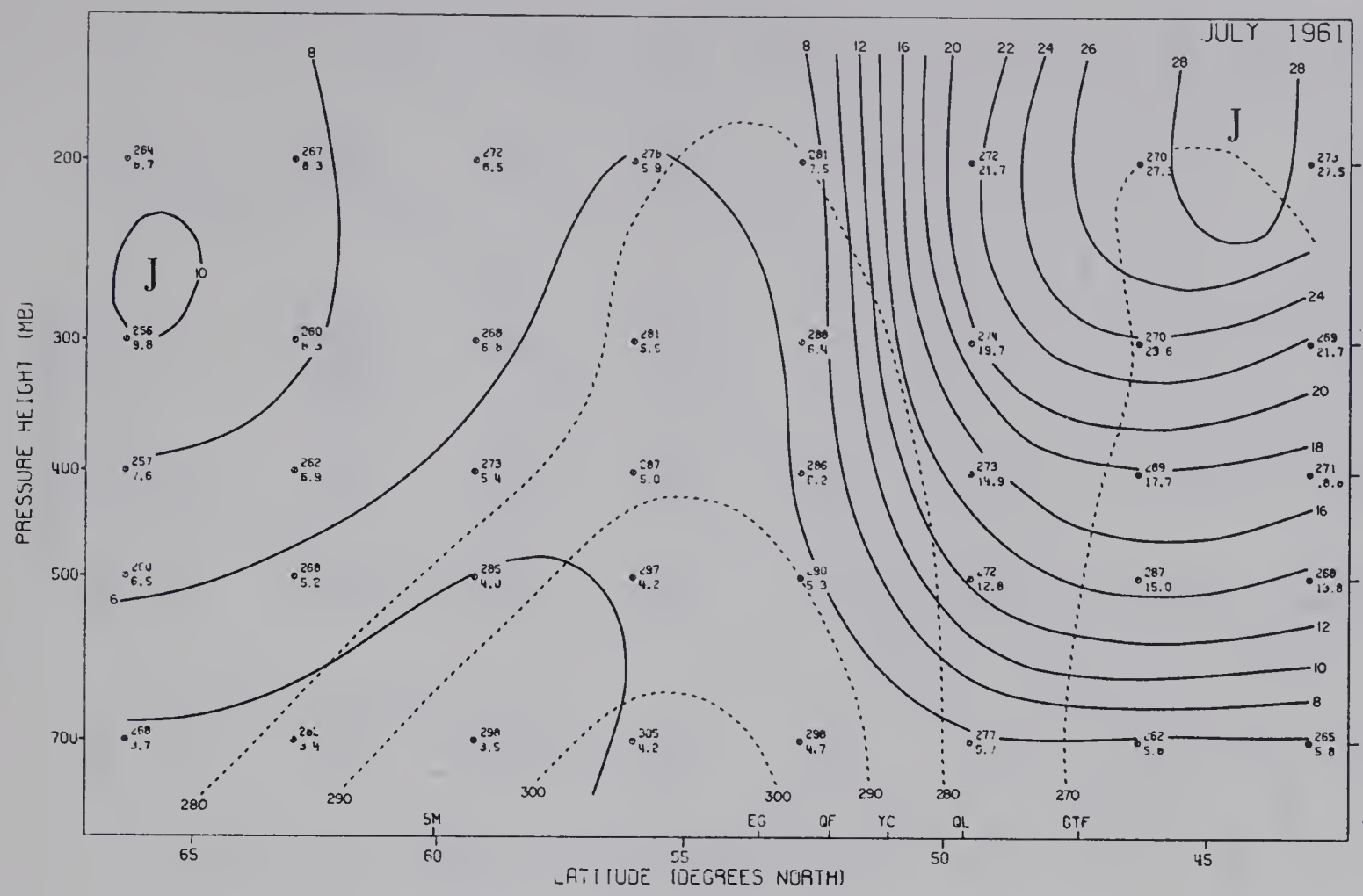

Fig. B-12 Monthly mean cross-sections for July and August, 1961.

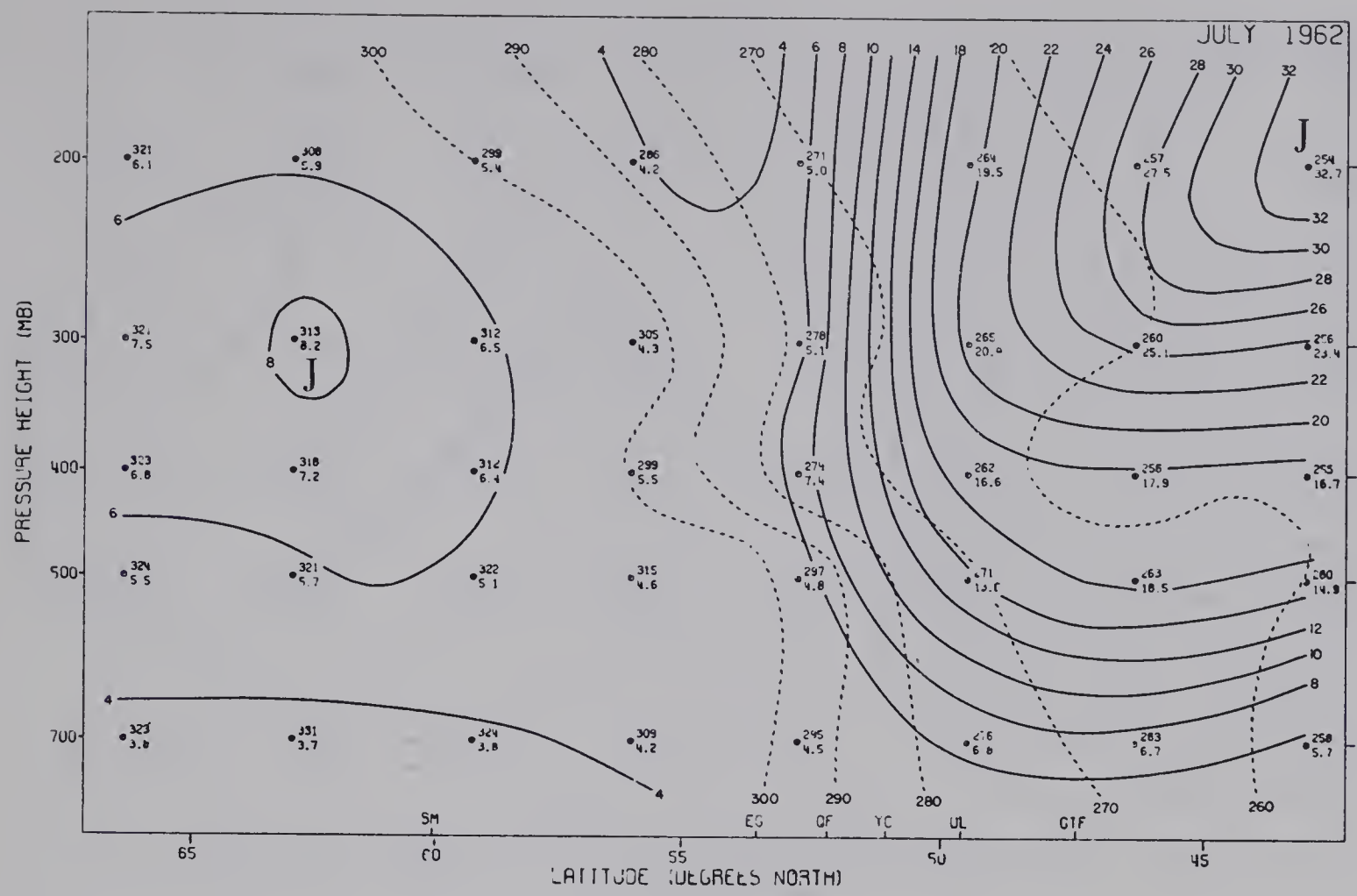

Fig. B-13 Monthly mean cross-sections for July and August, 1962.

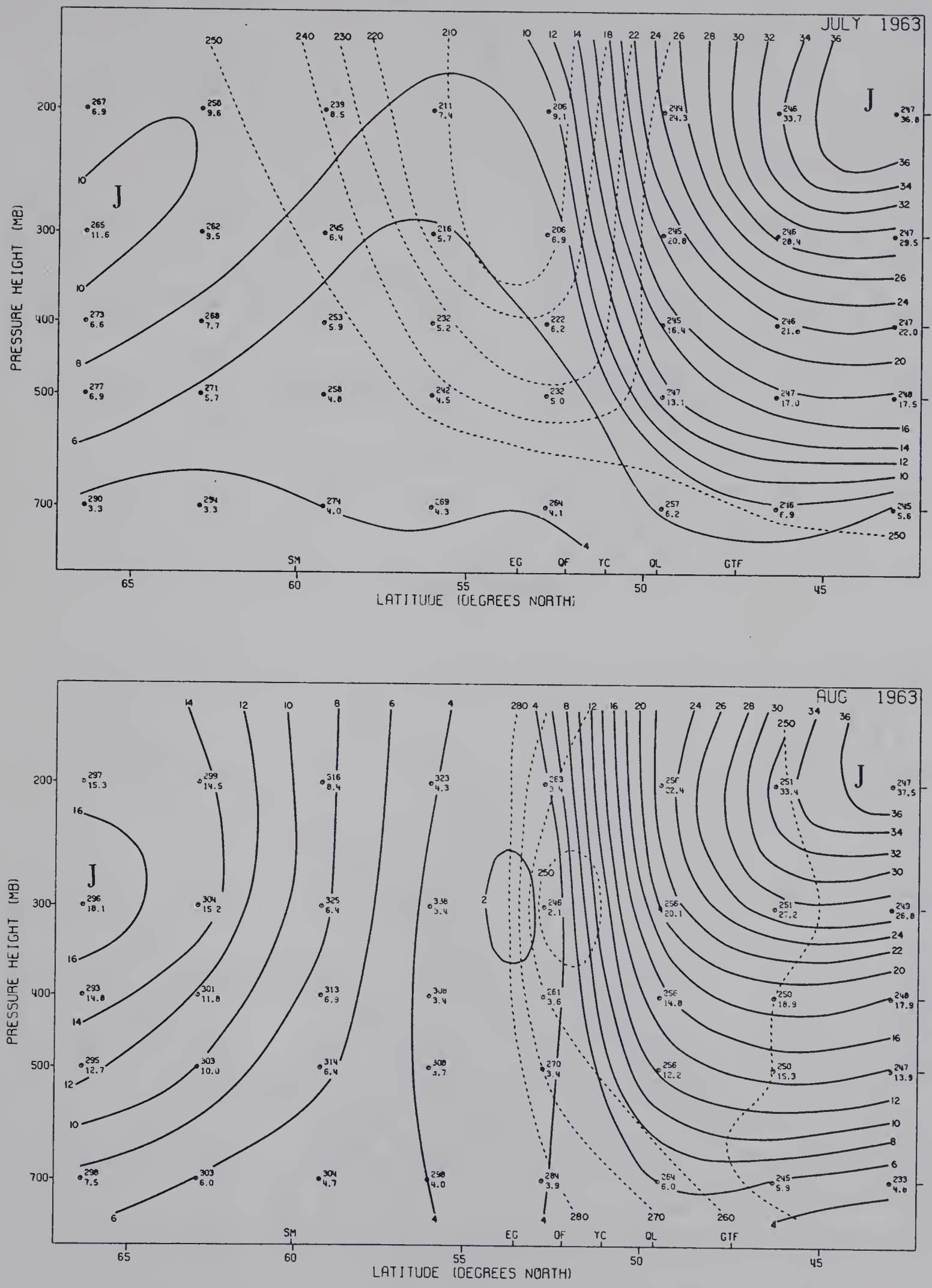

Fig. B-14 Monthly mean cross-sections for July and August, 1963.

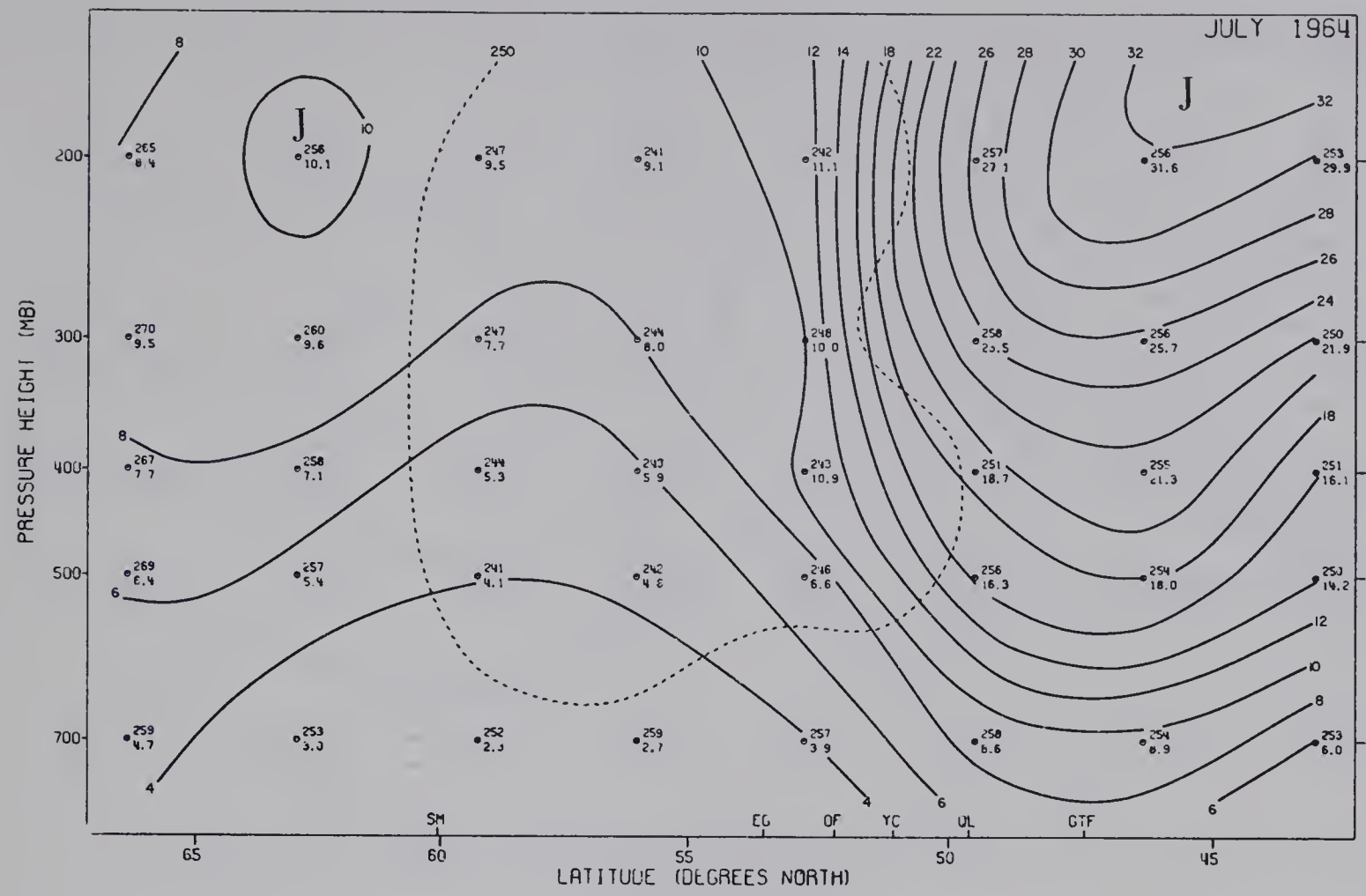

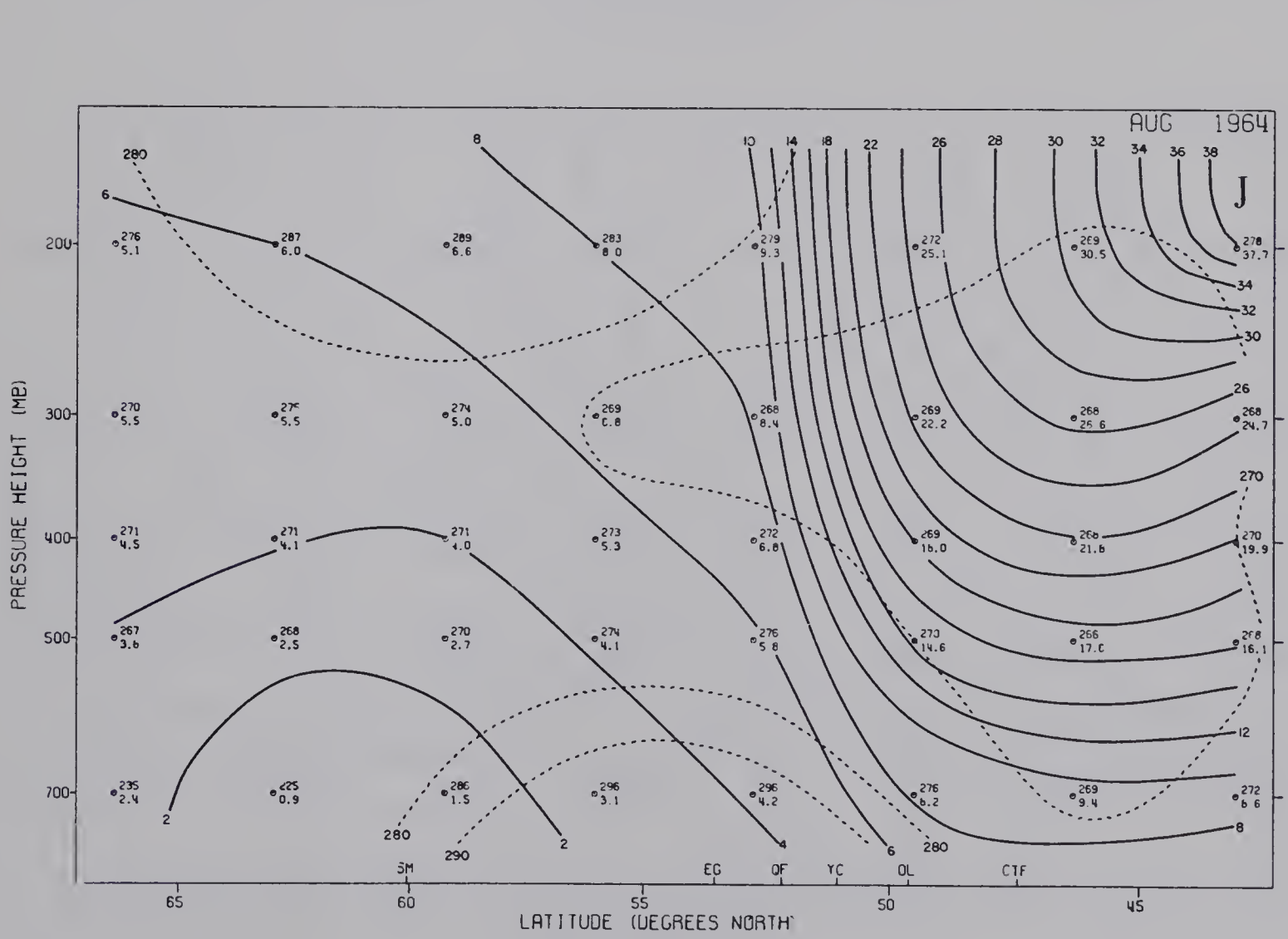

Fig. B-15 Monthly mean cross-sections for July and August, 1964.

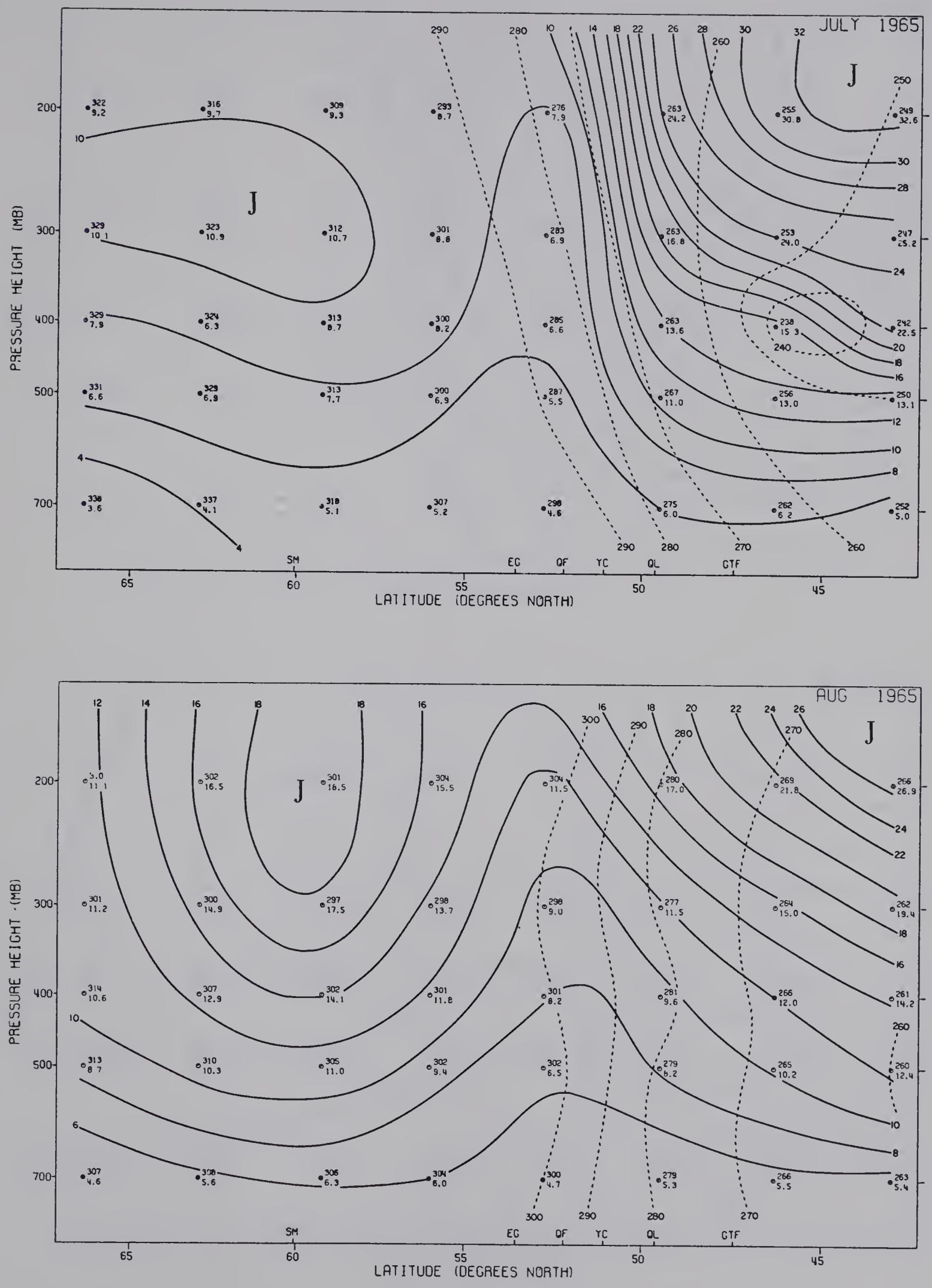

Fig. B-16 Monthly mean cross-sections for July and August, 1965.

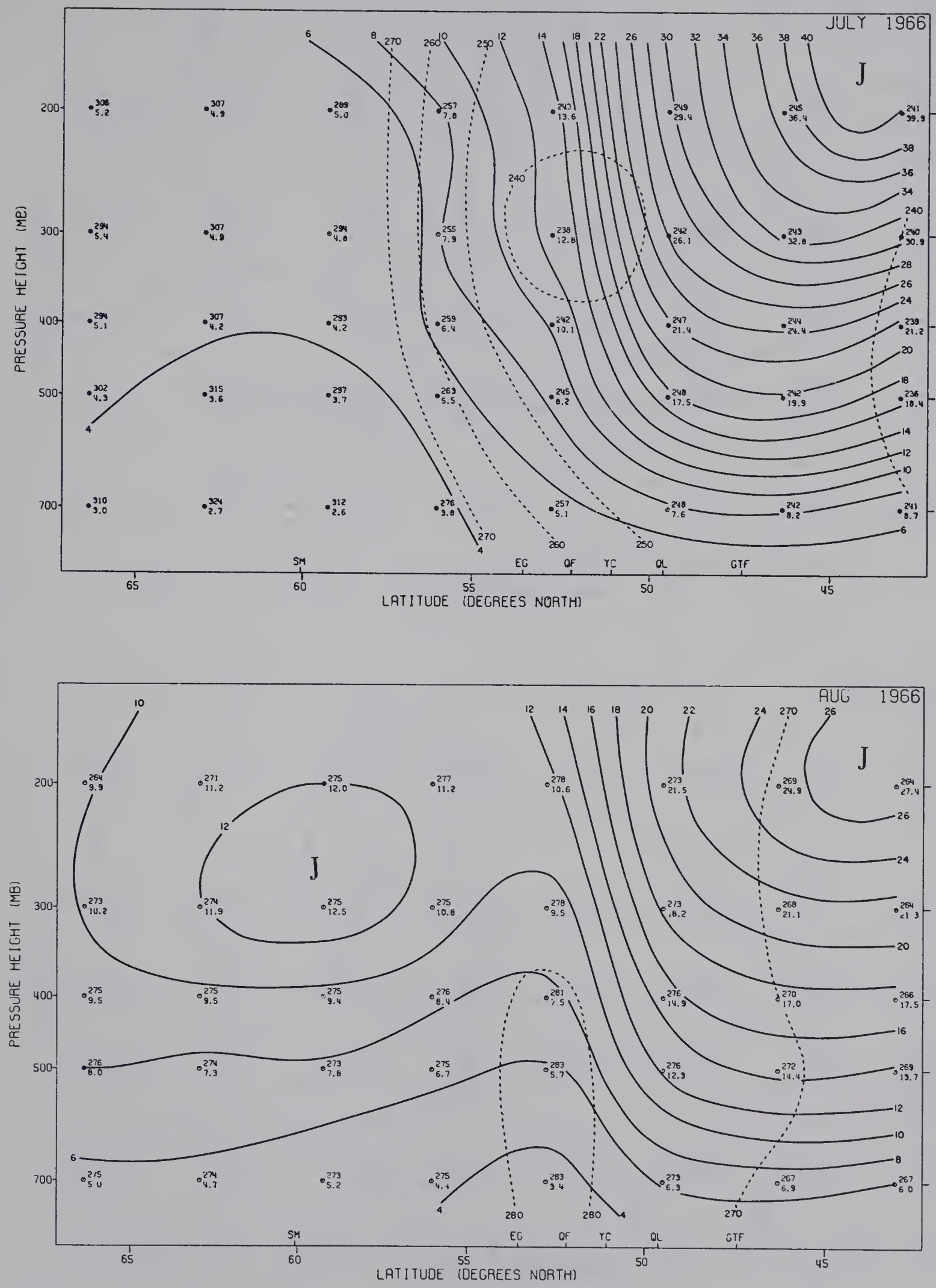

Fig. B-17 Monthly mean cross-sections for July and August, 1966.

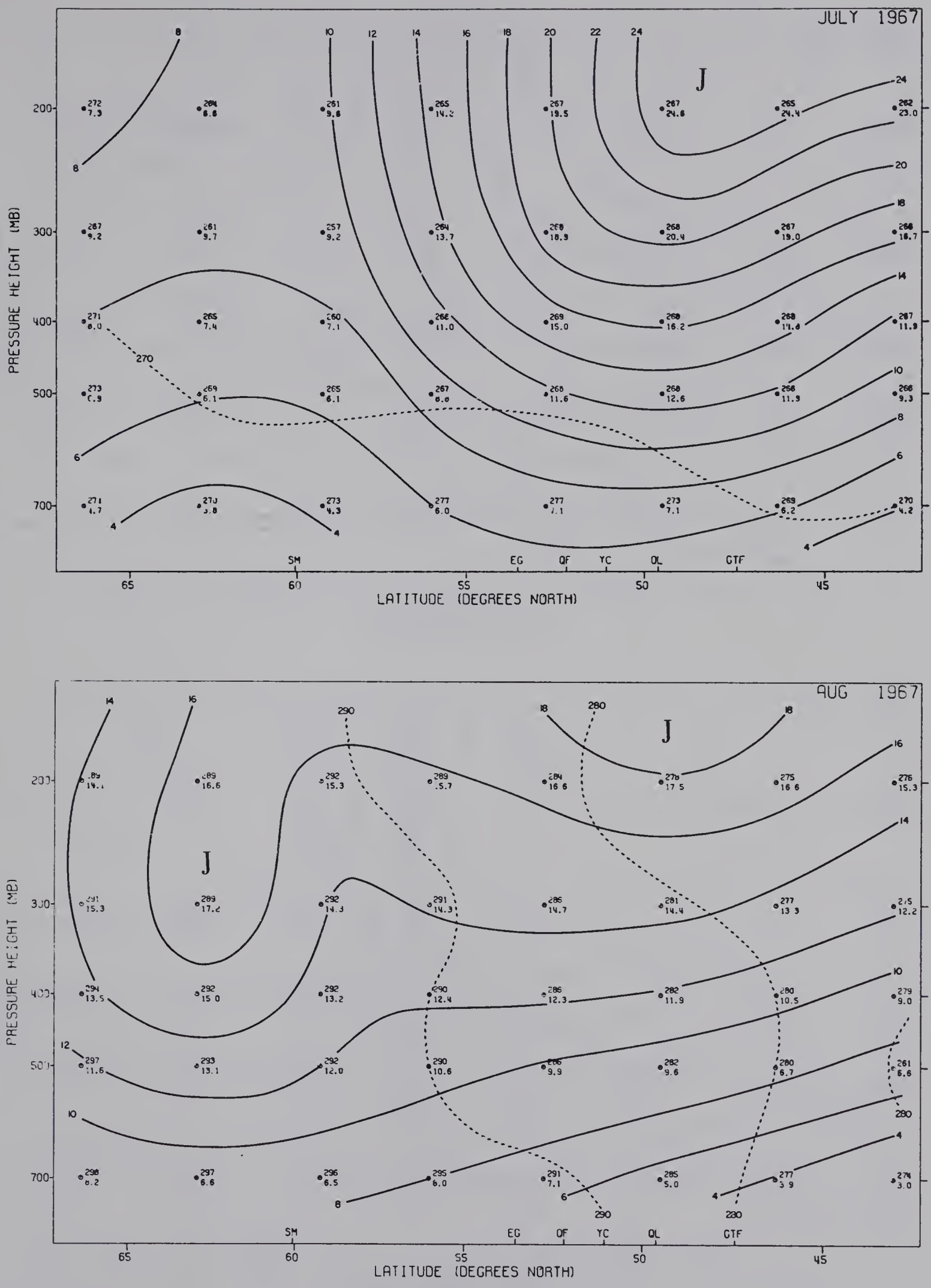

Fig. B-18 Monthly mean cross-sections for July and August, 1967.

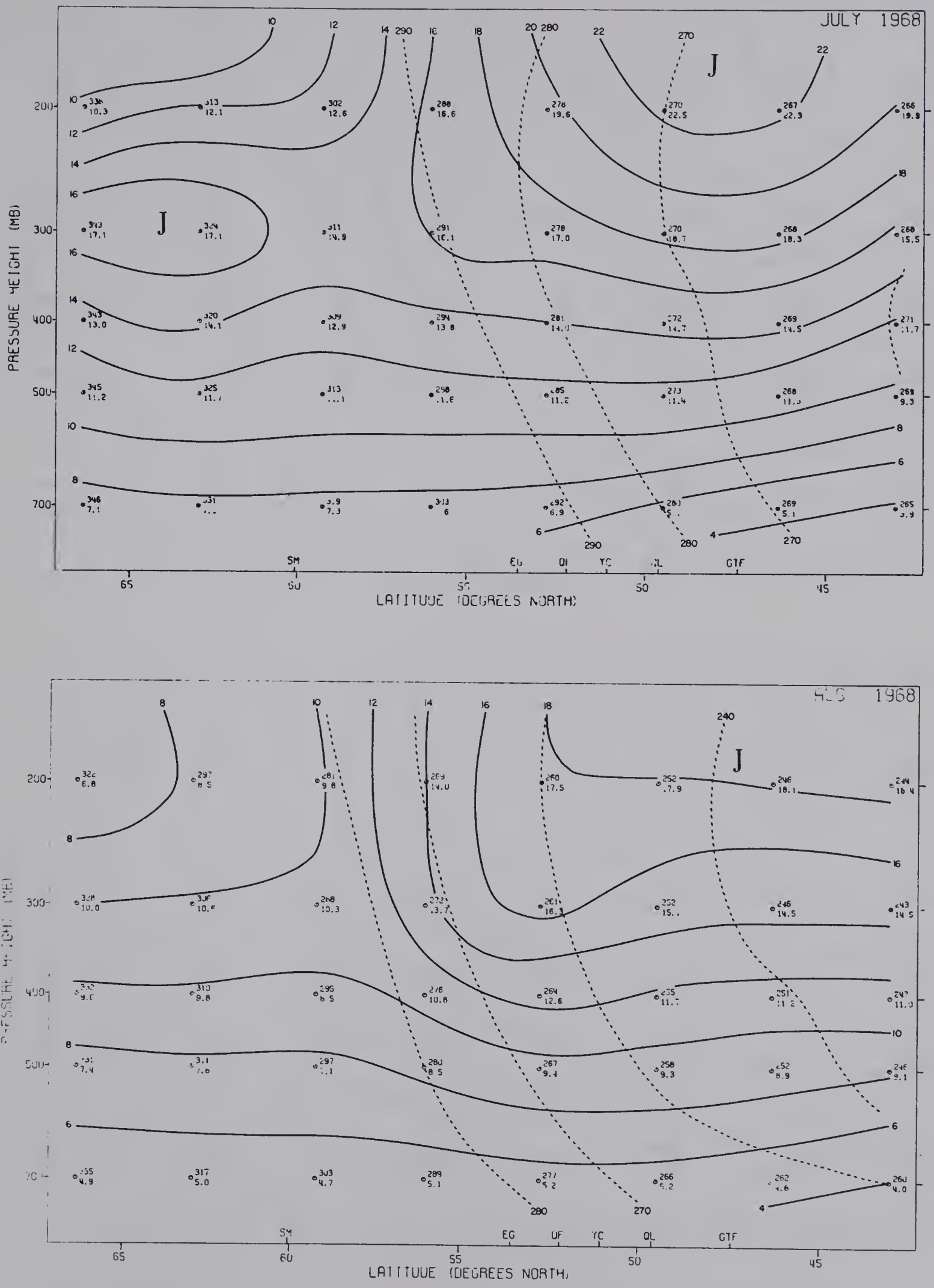

Fig. B-19 Monthly mean cross-sections for July and August, 1968.

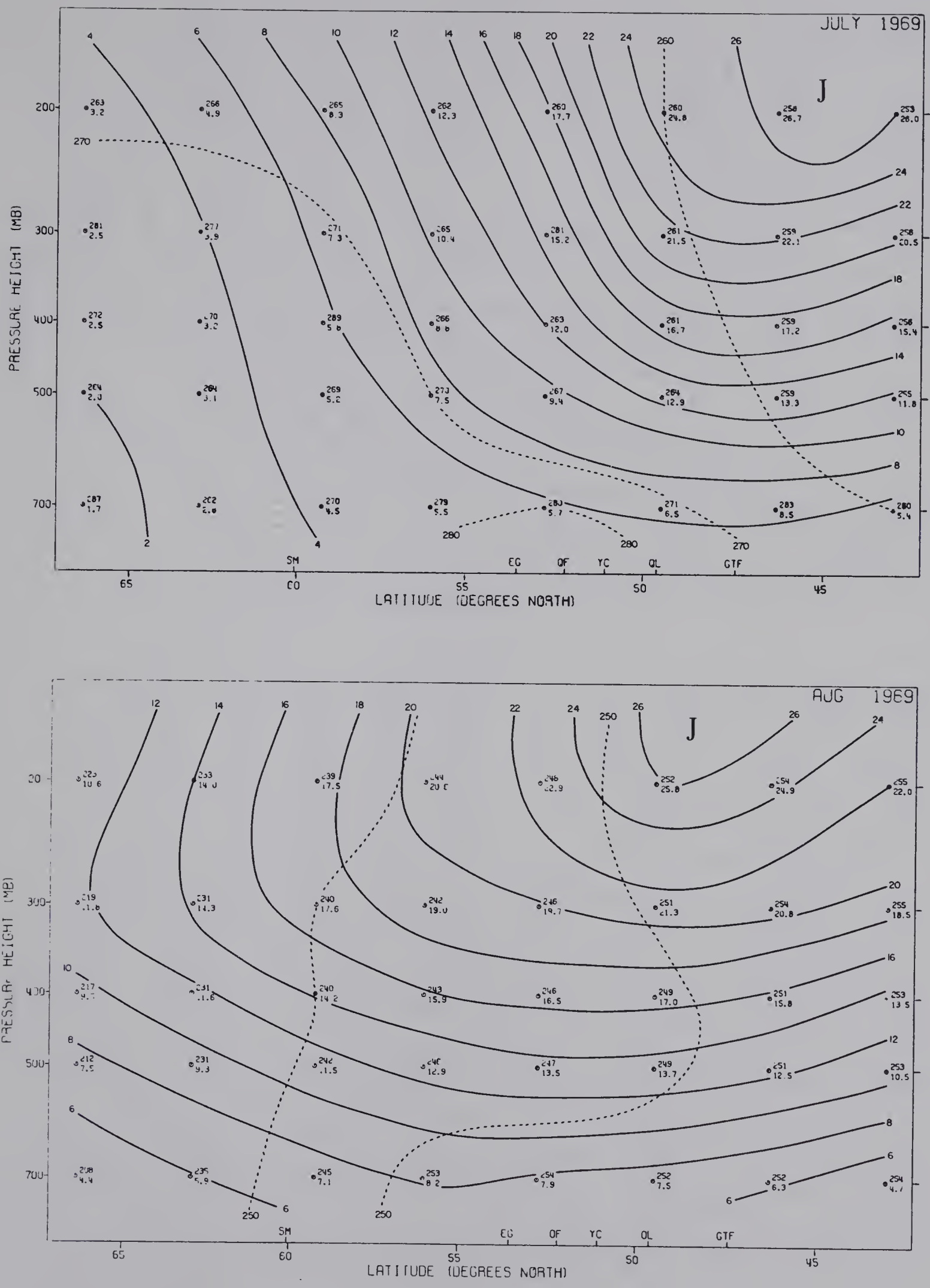

Fig. B-20 Monthly mean cross-sections for July and August, 1969.

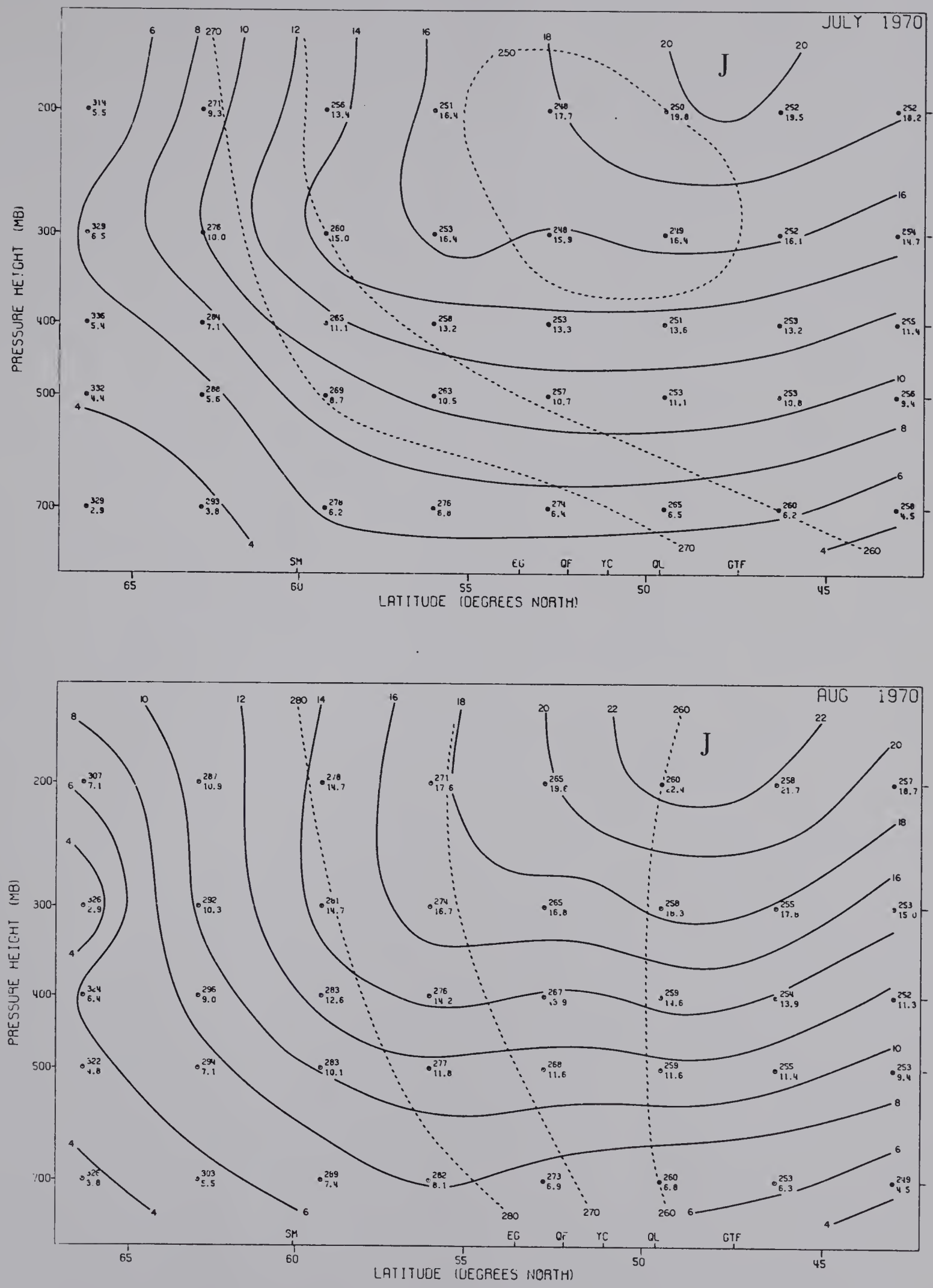

Fig. B-21 Monthly mean cross-sections for July and August, 1970.